

General Disclaimer

One or more of the Following Statements may affect this Document

- This document has been reproduced from the best copy furnished by the organizational source. It is being released in the interest of making available as much information as possible.
- This document may contain data, which exceeds the sheet parameters. It was furnished in this condition by the organizational source and is the best copy available.
- This document may contain tone-on-tone or color graphs, charts and/or pictures, which have been reproduced in black and white.
- This document is paginated as submitted by the original source.
- Portions of this document are not fully legible due to the historical nature of some of the material. However, it is the best reproduction available from the original submission.

REPORT

N71-12965

FACILITY FORM 602

(ACCESSION NUMBER)

51

(PAGES)

(THRU)

G3

(CODE)

(NASA CR OR TMX OR AD NUMBER)

32
(CATEGORY)

FASTENER LOAD ANALYSIS METHOD

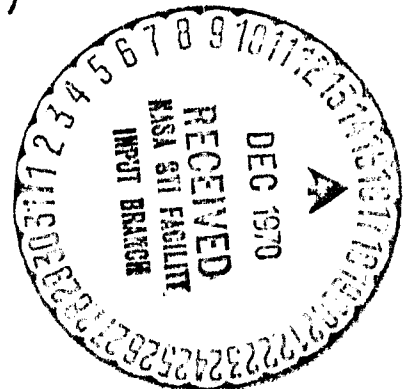
PHASE I REPORT

28 January - 1 August 1970

Contract No. ~~NAS8-25362~~

Control No. DCN-1-O-60-00081(1F)

MRI Project No. 3406-C



For

National Aeronautics and Space Administration
 George C. Marshall Space Flight Center
 Huntsville, Alabama 35812

32

FASTENER LOAD ANALYSIS METHOD

by

Fred R. Rollins, Jr.

PHASE I REPORT

28 January - 1 August 1970

Contract No. NAS8-25362
Control No. DCN-1-0-60-00081(1F)
MRI Project No. 3406-C

For

National Aeronautics and Space Administration
George C. Marshall Space Flight Center
Huntsville, Alabama 35812

PREFACE

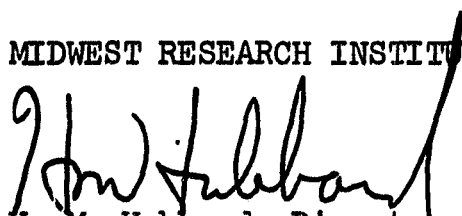
This report was prepared for the George C. Marshall Space Flight Center of the National Aeronautics and Space Administration under Contract No. NAS8-25362. The program was monitored by Mr. George Kurtz of the Marshall Space Flight Center.

The report covers work performed during the period 28 January to 1 August 1970. The objective of Phase I was to determine the feasibility of using ultrasonic techniques as an accurate tool for the analysis of bolt loads, primarily during tightening or assembly operations. The actual work has involved selection and development of a suitable technique plus a variety of tests and experiments designed to evaluate reproducibility and sources of error.

The subject project was conducted by Midwest Research Institute under the administrative supervision of Dr. H. M. Hubbard, Director of the Physical Sciences Division, and Mr. G. E. Gross, Head of the Physics Section. Mr. F. R. Rollins, Jr. served as project leader. Mr. Gerald Swanson provided valuable assistance in both program planning and experimental execution.

Approved for:

MIDWEST RESEARCH INSTITUTE


H. M. Hubbard, Director
Physical Sciences Division

7 August 1970

ssd

TABLE OF CONTENTS

	<u>Page</u>
Abstract	1
I. Introduction	2
II. Requirements and Technique Selection	3
III. The Frequency-Null Technique	5
IV. Preliminary Examination of Bolts	10
A. Transducer Coupling	16
B. Bolt-End Surface and Geometry	17
C. Length	18
D. Temperature	18
E. Plastic Yielding	22
F. Shear Stresses	26
G. Bending	26
V. NASA Supplied Bolts	29
VI. Potential Field Techniques	34
VII. Conclusions and Recommendations	39
Appendix A - Frequency-Null Response for Stressed Bolts	42
References	44

LIST OF FIGURES

<u>Figure</u>	<u>Title</u>	<u>Page</u>
1	Sketchs of Bolts Showing Effect of Stress	4
2	Block Diagram of Frequency-Null Interferometer	6
3	Oscillograms Showing Pulse Echo Pattern (Top), Same Pattern After Mixture With CW Signal (Center), and Expanded Sweep Presentation of Mixed Signal With Frequency Adjusted for Null Condition at First Echo	7

LIST OF FIGURES (Continued)

<u>Figure</u>	<u>Title</u>	<u>Page</u>
4	Bolt and Nut Diagrams Showing Relationships Between Total Length, l_t , and stressed lengths, l_s and $l_{s'}$, for Totally Threaded Bolts (1a) and Partially Threaded Bolts (1b).	9
5	NASA Supplied Bolts	11
6	Bolts Purchased Locally for Frequency-Null Inspection	12
7	MRI-1 Aluminum Bolt With Transducer Held in Place With Yoke Arrangement	14
8	Frequency Change vs. Bolt Load for Three MRI Bolts.	15
9	Response Curves for an Aluminum Bolt With Indicated Stressed Length	19
10	Response Curves for Two Aluminum Bolts of the Same Stressed Length but With Different Real Length as Indicated	20
11	Changes in Null Frequency Versus Temperature for Two NASA Supplied Bolts	21
12	Frequency Change Versus Load for an (MRI-1) Aluminum Bolt Held at the Indicated Temperatures During the Loading Operation	23
13	Loading and Unloading Curves for an Aluminum Bolt Stressed Beyond the Yield Strength	24
14	Frequency Change Versus Load for Three Identical 3/4-In. Aluminum Bolts Loading in (A) Pure Tension, (B) Torque-Tension With Threads Lubricated and (C) Torque-Tension Without Lubrication.. . . .	25
15	Frequency-Versus-Load Curves for an Aluminum Bolt With (A) 0 Mils, (B) 10 Mils, (C) 20 Mils, and (D) 30 Mils of Steel Shimstock Under one Side of the Bolt Head to Induce Bending During the Loading Operation	27

LIST OF FIGURES (Concluded)

<u>Figure</u>	<u>Title</u>	<u>Page</u>
16	Frequency Change Versus Load for Four NASA-Supplied Bolts. .	30
17	Frequency Change Versus Load for Several Different Bolt Sizes and Alloys	31
18	Normalized Frequency Change Versus Stress for NASA-Supplied Bolts	32
19	Frequency Change Versus Stress for 3/8-In. and 3/4-In. Bolts of 4140 Steel	33
20	Frequency Change Versus Load for 3/4-In. Aluminum Bolt, AN 12DD-H35A, and 3/4-In. Tool Steel Bolt, NAS 1312-29.. .	35
21	Prototype Socket Wrench With Spring Loaded Transducer (Top) and Modified Socket Wrench With Electrical Contact for Separate Transducer (Bottom)	36
22	Photograph of Bolt Being Tightened in Torque Tension Tester and the Load Being Analyzed With the Frequency-Null Equipment	38

LIST OF TABLES

<u>Table</u>	<u>Title</u>	<u>Page</u>
1	Information on Bolts Investigated.	13

ABSTRACT

This report covers a preliminary investigation into the feasibility of analyzing bolt loads by ultrasonic techniques. Various techniques were evaluated and an interferometric method, called frequency nulling, was selected for experimental testing. In agreement with theoretical predictions the frequency-null response was found to be linearly related to tensile stresses oriented parallel to the bolt axis. Under rather idealized conditions bolt loads can be determined with errors of less than 1%. The ultimate operational accuracy depends on a number of variables, such as bolt dimensions and geometry, temperature, uniformity of stresses, and bolt materials, but load analysis to within $\pm 3\%$ is achievable without too much difficulty. Best results are obtained with the ultrasonic transducer contact coupled to the bolt head, and this is facilitated by having a small flat area near the center of the bolt head. The transducer can be applied without interfering with normal wrenching operations.

I. INTRODUCTION

It has been known for some time that stresses, both applied and residual, can produce small changes in the velocity of propagation of ultrasonic waves traveling through metals and certain other solids.^{1,2/} These stress-induced velocity effects are relatively small when compared to velocity changes due to other variables, such as alloy differences or preferred grain orientation. Because the stress effect is relatively weak it has not found widespread use in stress analysis applications even though considerable research has been directed toward this end, particularly in regard to the analysis of residual stresses. This program was initiated to determine the feasibility of using stress-induced changes in ultrasonic propagation parameters in analyzing the load on aerospace fasteners, particularly threaded bolts.

There are two distinctly different applications for an ultrasonic load analyzer. The first application involves the analysis of load or stress levels during actual assembly, i.e. while the bolt is being tightened. In this application we might think of the ultrasonic measurement as a substitute for torque wrench readings. Since ultrasonic techniques will probably be more complicated, they must have significant advantages, such as improved accuracy, if they are to be used over the torque wrench, which often exhibits errors of $\pm 25\%$.

The second potential application of ultrasound to bolt load analysis is in evaluating the post-assembly load, i.e., perhaps weeks or months after assembly and possibly after exposure to various environments including intense vibration. In this application the torque wrench is of little value unless the bolts can be loosened and retorqued. At the present time there is no satisfactory answer to the post-assembly load analysis problem.

The two analysis problems discussed above also place very different requirements on an ultrasonic system. In this program, major emphasis has been placed on load analysis during assembly, but the post-assembly problem has been investigated also.

This report contains further discussion of load analysis problems together with results obtained during the first six months of the program. As expected, the ultrasonic results are very dependent on the geometry of both the head and threaded end of a given bolt configuration. It has been shown that under rather idealized conditions ultrasonic measurements can be related to bolt loads with errors of approximately $\pm 1\%$. The errors increase as the idealized conditions degenerate, but loads have been measured on some "as received" bolts with errors of less than $\pm 5\%$. The latter

results were obtained using only tools consistent with normal bolt tightening procedures plus necessary electronic instrumentation.

II. REQUIREMENTS AND TECHNIQUE SELECTION

As mentioned in the introduction, the velocity of ultrasonic waves in a metal is influenced slightly by superimposed stresses. Some techniques, based on ultrasonic shear waves,^{3/} can be used to evaluate stress-induced velocity changes without any additional influence from the dimensional changes which normally accompany the stress. However, such techniques are not readily applicable to the fastener load problem. In this problem it is difficult to separate velocity and length effects so we have chosen to evaluate the combined effect of both length and velocity. Consider the bolt sketches shown in Figure 1. The bolt is stretched in normal applications where the tensile stress within the bolt counteracts some external force. The overall length increases by some increment Δl and the velocity in the stressed region may change by an increment Δv , which we will assume can be either positive or negative. Although we are primarily interested in the stressed region, we are forced to examine ultrasonic parameters which are also influenced by metal outside of the stressed region. For example, assume that the round trip transit time of an ultrasonic pulse is to be evaluated as the pulse travels from the bolt head to the threaded end and back to the head. The transit time in the stressed bolt is dependent on both Δl and Δv . We can assume that $\frac{\Delta l}{l}$ is less than the strain produced by yield point stresses, i.e., approximately 0.2%. Previous measurements^{2/} suggest that $\frac{\Delta v}{v}$ is of the same order of magnitude. Thus, the fractional change in transit time, $\frac{\Delta T}{T}$ can be estimated to be in the range 10^{-2} to 10^{-3} . Adequate measurement of such small changes normally requires techniques with errors of less than 1 part in 10^4 to 10^5 , considerably beyond standard pulse-echo transit time measurements. Some form of ultrasonic interferometry is usually necessary for such accuracies.

During the early phases of this program, preliminary experiments were performed to confirm the magnitude of the expected effect and to demonstrate that interferometric techniques could be applied to the problem. A literature search was made to uncover all potential techniques, of which the most promising were selected for further study and experimentation. The techniques which received primary study included the two-specimen interferometer,^{4/} pulse superposition,^{5/} pulse-echo overlap,^{6/} and an interferometric method first described by Pervushin and Filippov,^{7/} but subsequently modified by Benson and Associates^{8/} and called the frequency-null technique. All of these techniques theoretically have sufficient accuracy for the bolt load analysis problem so final selection was primarily based on relative simplicity and applicability to ultimate field type testing. The two-specimen

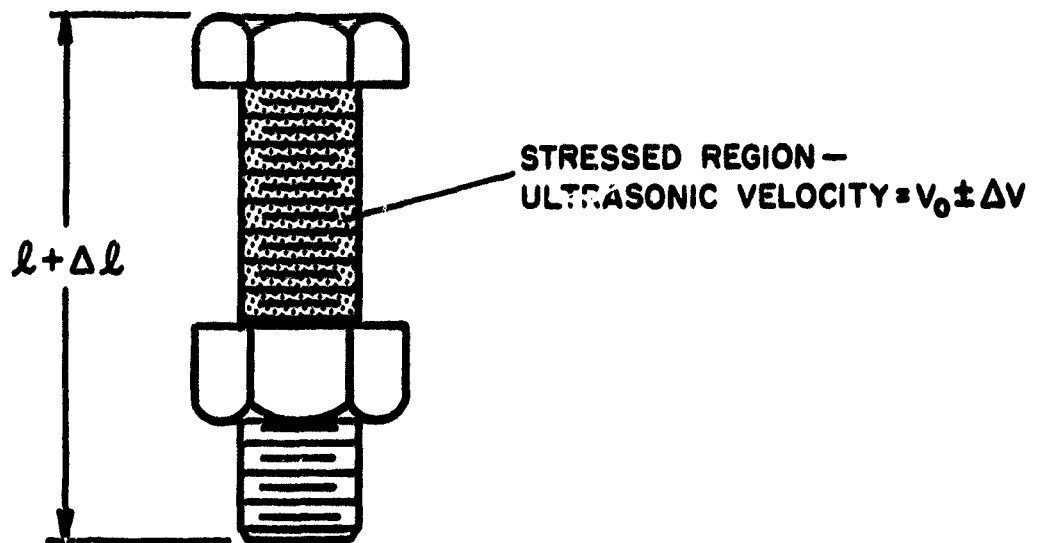
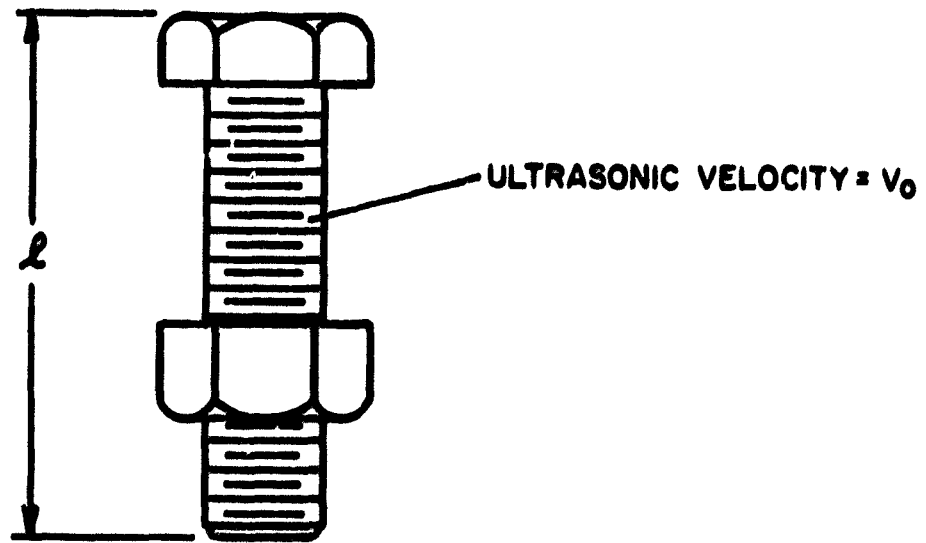


Figure 1 - Sketchs of Bolts Showing Effect of Stress

interferometer does not yield continuous readings as readily as the frequency-null technique; furthermore, it requires a relatively large number of echos whereas the frequency-null technique requires only one echo. Multiple echos (at least two) are also required for both the pulse superposition and pulse-echo overlap technique. There are several advantages in using only the first echo. Generally the first echo is the strongest (in fact, it may be the only one available) and is less complicated by interference with unwanted noise. Thus, a modified frequency-null technique was selected for major experimental testing and is described below.

III. THE FREQUENCY-NULL TECHNIQUE

A block diagram of our instrumentation for the frequency-null technique is shown in Figure 2. The signal generator provides a variable frequency CW signal which is fed to a frequency counter and a gated amplifier. The gated rf pulse from the amplifier drives the piezoelectric transducer which is coupled to one end of the bolt under investigation. Using this arrangement, the frequency of the rf pulse is controlled at the signal generator and can be accurately determined by the frequency counter. The electrical signals created at the transducer by ultrasonic echoes from the opposite end of the bolt are then fed through a TR switch to one input of a differential preamplifier on the oscilloscope. The TR switch is utilized to reduce saturation in the preamplifier by blocking passage of the large driving pulse and permitting the weaker echos to pass. Part of the CW signal from the signal generator serves as the other input to the differential preamplifier where it is ultimately mixed with the echo signals from the bolt.

Any of the pulse echoes can be utilized in taking data but we emphasized use of the first echo because it is less likely to be confused by unwanted signals from side wall reflections, beam spreading, slower modes, etc. Data are obtained by varying the frequency and amplitude of the first echo until almost complete destructive interference between the CW and pulsed signal is observed on the oscilloscope. The frequency as determined by the counter is then recorded. If a stress is applied to the bolt the frequency must be varied in order to maintain the interference, or null, condition.

Oscillograms showing various echo patterns and frequency null presentations are shown in Figure 3. The top oscillogram is simply the pulse echo pattern from an aluminum bolt. The center photo shows the same pattern after mixing with the CW signal. The bottom photo shows the mixed pattern at an expanded sweep and with the frequency adjusted for null conditions at the first echo. Clean echos such as those shown in Figure 3

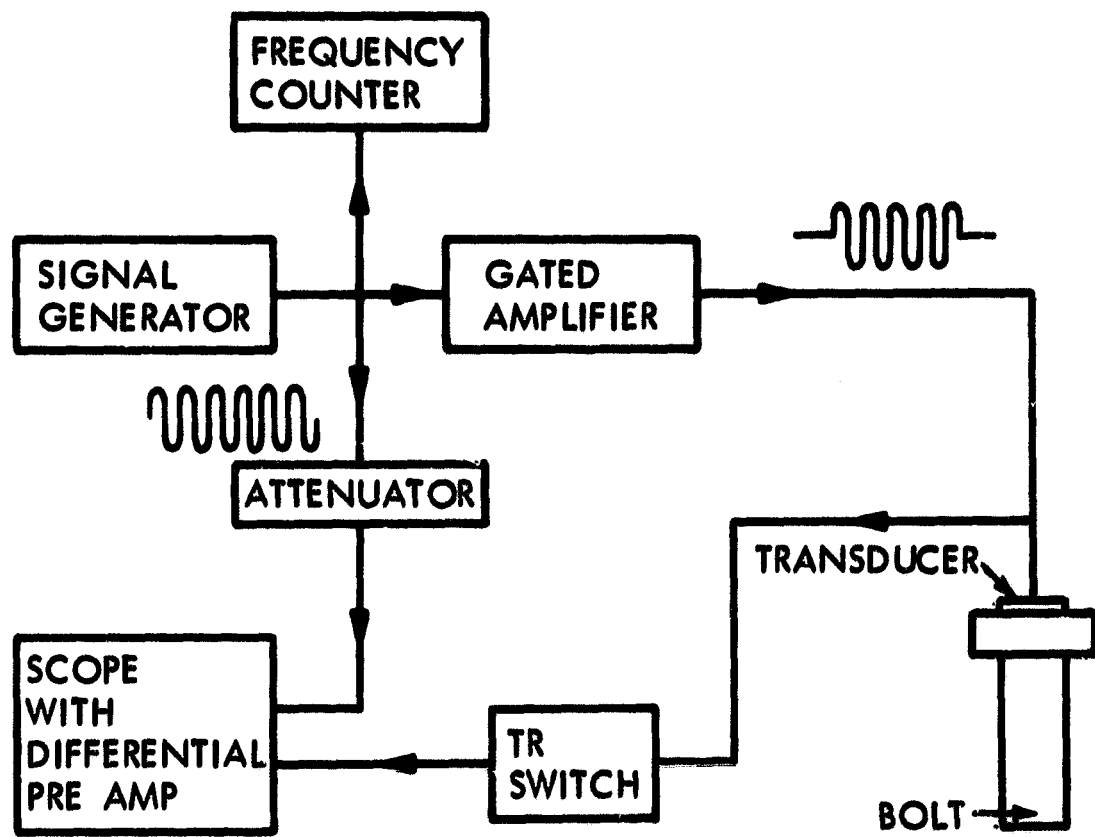


Figure 2 - Block Diagram of Frequency-Null Interferometer

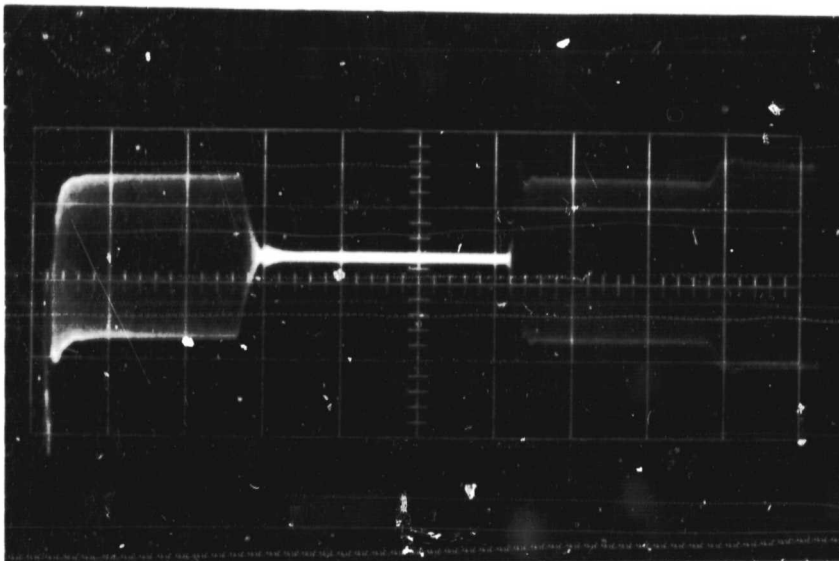
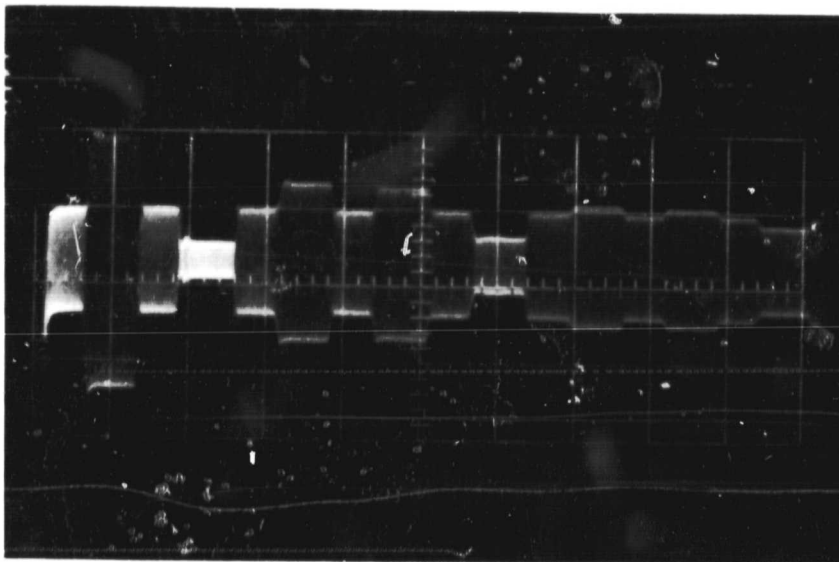
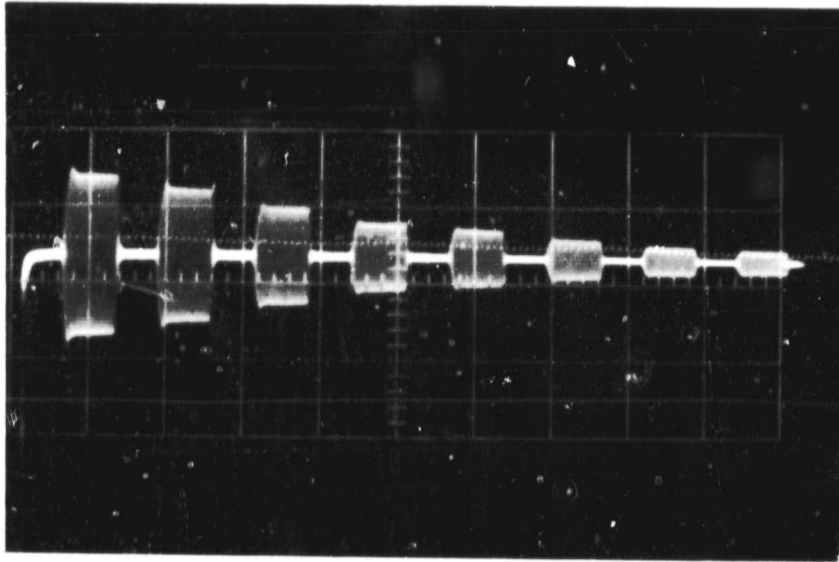


Figure 3 - Oscillograms Showing Pulse Echo Pattern (Top), Same Pattern After Mixture of CW Signal (Center), and Expanded Sweep Presentation of Mixed Signal with Frequency Adjusted for Null Condition at First Echo

can be reproducibly nulled with frequency variations of less than 100 Hz. Assuming a typical CW frequency of 10 MHz it is clear that a given null frequency can be determined with an error of about 1 part in 10^5 .

As mentioned previously the frequency required to maintain a given null condition varies with the stress or load on the bolt. Appendix A includes a simple derivation for the interdependence between the null frequency and the stress or load condition. For bolts which are threaded over the full length (see Figure 4a), the expression relating the fractional change in frequency, $\frac{\Delta f}{f}$, and the stress, S, is as follows:

$$\frac{\Delta f}{f} \cong \frac{l_s}{l_t} (\beta/2 - \alpha) S \quad (1)$$

where l_t is the total length of the bolt and l_s is the length subjected to stress (defined approximately as the distance between the head and nut as shown in Figure 4a). The term, $(\beta/2 - \alpha)$, is a constant for a given material but differs from one metal to another. Beta is a complex term containing material constants which define the stress-induced change in velocity, whereas α is simply the reciprocal of Young's modulus and defines the stress-induced change in length. Expression (1) is strictly valid only for stresses below the yield strength. Thus, in the elastic region Δf should be linearly related to stress.

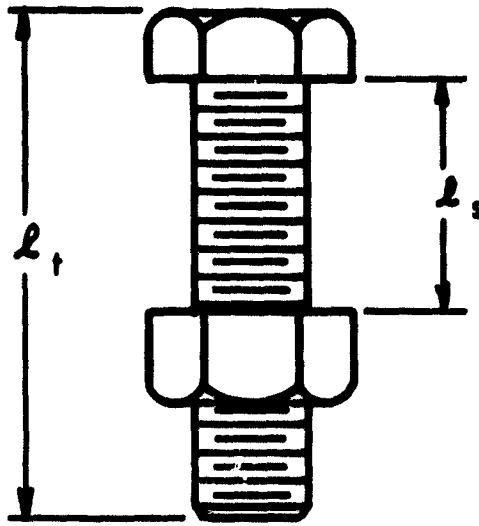
Expression (1) is also based on a uniform stress over the length l_s . However, in a partially threaded bolt, such as that shown in Figure 4b, it is clear that l_s is divided into two distinct stress areas. Since the effective diameter of the threaded area is less than that of the unthreaded area, the stress will be greater in the threaded portion. It is a simple task to modify Expression (1) to include two stressed lengths, l_s and $l_{s'}$, subject to stresses S and S', respectively. The result is

$$\frac{\Delta f}{f} \cong \frac{(\beta/2 - \alpha)}{l_t} (S l_s + S' l_{s'}) \quad (2)$$

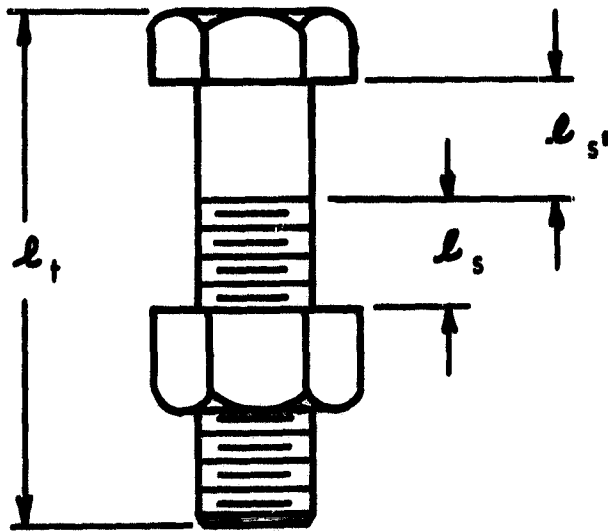
Since the stress in each sublength is related to the overall load, L, and the effective cross-sectional area A, we can further modify (2) as follows:

$$\frac{\Delta f}{f} \cong \frac{(\beta/2 - \alpha)}{l_t} \left(\frac{l_s}{A_s} + \frac{l_{s'}}{A_{s'}} \right) L \quad (3)$$

Thus $\Delta f/f$ is still linear in L, but for a given alloy and load, we see that $\Delta f/f$ also depends on five dimensions, all of which must be considered in determining the desired Δf value for a particular bolt application.



(1a)



(1b)

Figure 4 - Bolt and Nut Diagrams Showing Relationships Between Total Length, l_t , and stressed lengths, l_s and $l_{s'}$, for Totally Threaded Bolts (1a) and Partially Threaded Bolts (1b).

It should be emphasized that when the frequency is varied over a wide range many null conditions are observed. From Appendix A one can see that nulls occur each time an integral number of wavelengths fit into the bolt length. When we follow the frequency of a particular null, while a bolt is being loaded, we are maintaining the same number of wavelengths within the bolt. The resulting Δf is the quantity previously referred to in Expressions (1)-(3).

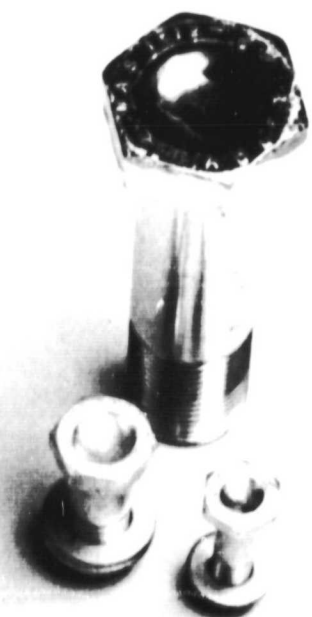
There is another variable which can be obtained using the frequency-null technique. It also is a frequency difference, which we will identify as ΔF . This frequency difference is obtained by evaluating the frequencies of two adjacent nulls, i.e., two interference conditions represented by n and $n+1$ wavelengths within the specimen. The value of ΔF is simply related to the total transit time, T as follows: $\Delta F = 1/T$. At first glance it appears that a measurement of ΔF might also be a very convenient way of evaluating bolt loads, since the transit time does vary with load. However, there is an accuracy problem in this kind of measurement. The round trip transit time for a 2 in. long bolt would be approximately 20 μ sec. Thus, ΔF_0 would be about 50 KHz. If the transit time is now changed from T_0 to T_s by stress application the value of ΔF_s will vary from 50 KHz by an amount equal to about 1 part in 10^2-10^3 , or 500 to 50 Hz. As mentioned previously a given null can only be reproduced to about 100 Hz so the errors are almost as large as the quantity of interest, namely $(\Delta F_0 - \Delta F_s)$. The accuracy can be improved somewhat by scanning across many nulls; let us assume 10. Then, $(\Delta F) \times (10) \cong 500$ KHz, and the quantity $(\Delta F_0 - \Delta F_s) \times 10$ becomes 500 to 5,000 HZ, but the error is still about 200 HZ. All this simply shows that the relative frequency changes for a particular null can be determined much more accurately than the absolute transit time.

IV. PRELIMINARY EXAMINATION OF BOLTS

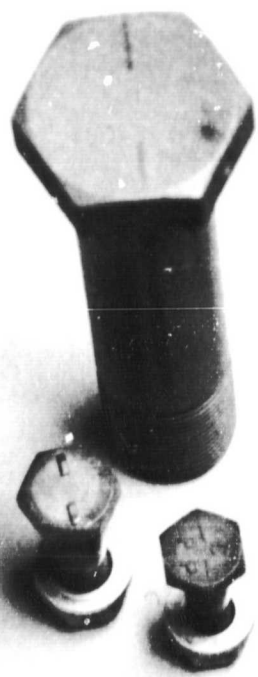
The bolts which have been examined during Phase I of this program are shown in Figures 5 and 6. Those shown in Figure 5 were supplied in limited numbers by the Marshall Space Flight Center and are further described in Table I. The bolts of Figure 6 were purchased locally in quantity for tests that required large numbers of specimens. Many of our preliminary tests were performed using the 3/4 in. aluminum bolt configuration shown in Figure 6 and designated MRI-1. Direct coupling of a transducer to the head of these bolts was made difficult by a small raised "bump" in the center. After removal of the bump with emery paper satisfactory echo patterns were achieved at a frequency of 10 MHz. Small commercial transducers were first coupled to the bolt head using silicone vacuum grease and a holding fixture as shown in Figure 7. Using this type of arrangement with the bolts loaded in a Skidmore-Wilhelm torque-tension tester, Δf -versus-load data were obtained similar to those shown in Figure 8.



4140 STEEL



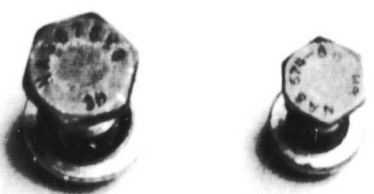
TOOL STEEL



ALUMINUM



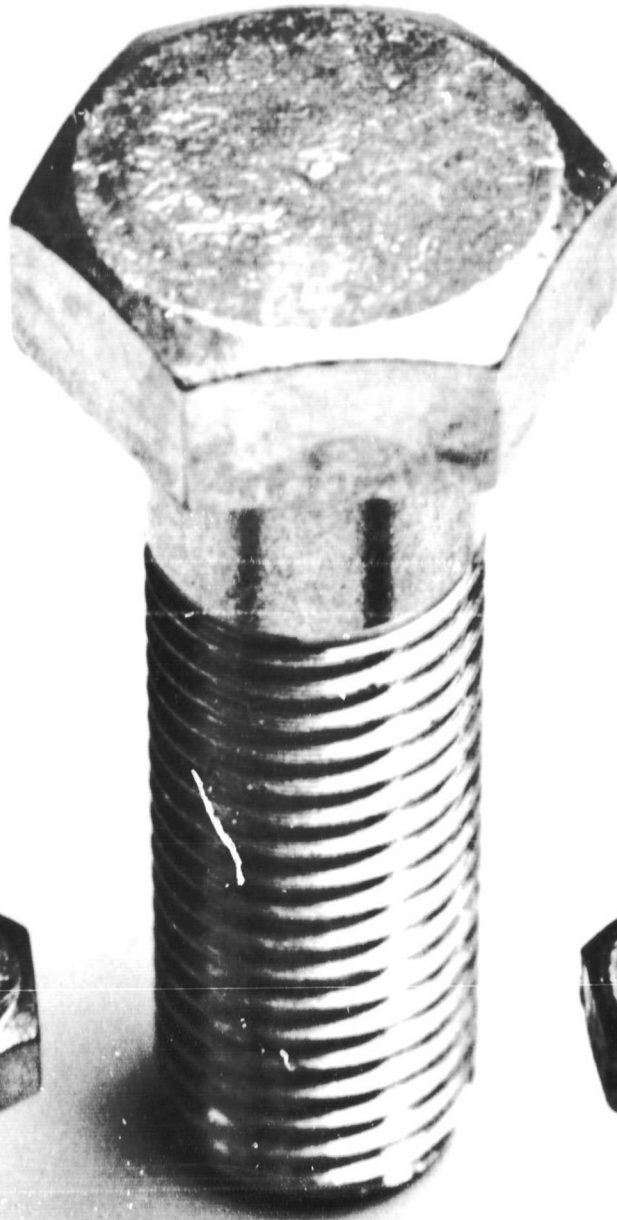
431 STAINLESS



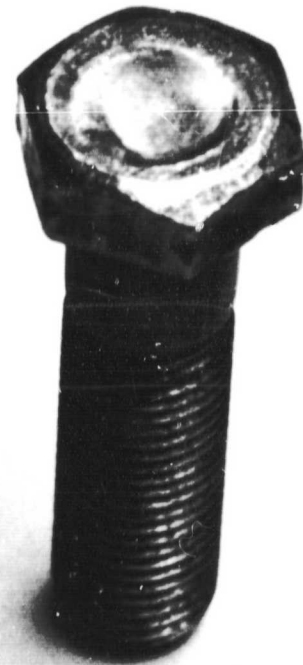
6-4 TITANIUM

Figure 5 - NASA Supplied Bolts

MRI-1 ALUMINUM



MRI-3
STAINLESS



MRI-2
MILD STEEL

Figure 6 - Bolts Purchased Locally for Frequency Null Inspection

TABLE I

INFORMATION ON BOLTS INVESTIGATED

<u>Code Number</u>	<u>Size</u>	<u>Material</u>	<u>Ultimate Tensile Strength of Material</u>	<u>Configuration</u>	<u>Comments</u>
NAS 676 V8	3/8 x 1.078	6-4 Titanium	~ 158,000 psi	Hex	
NAS 674 V8	1/4 x 0.925	6-4 Titanium	~ 158,000 psi	Hex	
AN 12DD-H35A	3/4 x 3.781	Aluminum	~ 60,000 psi	Hex	Drilled Head
AN 5DD-11A	5/16 x 1.219	Aluminum	~ 60,000 psi	Hex	
AN 4DD-10A	1/4 x 1.031	Aluminum	~ 60,000 psi	Hex	
AN 12C-36A	3/4 x 3.906	431 Stainless	~ 120,000 psi	Hex	
AN 6C-14	3/8 x 1.578	431 Stainless	~ 120,000 psi	Hex	Drilled Shank
AN 4C-10	1/4 x 1.032	431 Stainless	~ 120,000 psi	Hex	Drilled Shank
MS 20012-32	3/4 x 3.062	4140 Steel	~ 160,000 psi	Int. Wrench	
MS 20006-14	3/8 x 1.562	4140 Steel	~ 160,000 psi	Int. Wrench	
MS 20004-10	1/4 x 1.125	4140 Steel	~ 160,000 psi	Int. Wrench	
NAS 1312-29	3/4 x 2.853	Tool Steel	~ 160,000 psi	Hex	Spherically recessed heads
NAS 1306-12W	3/8 x 1.078	Tool Steel	~ 160,000 psi	Hex	
NAS 1304-8W	1/4 x 0.925	Tool Steel	~ 160,000 psi	Hex	
MRI-1	3/4 x 3.00	Aluminum		Hex	
MRI-2	3/8 x 1.75	Mild Steel		Hex	
MRI-3	3/8 x 1.75	Stainless		Hex	

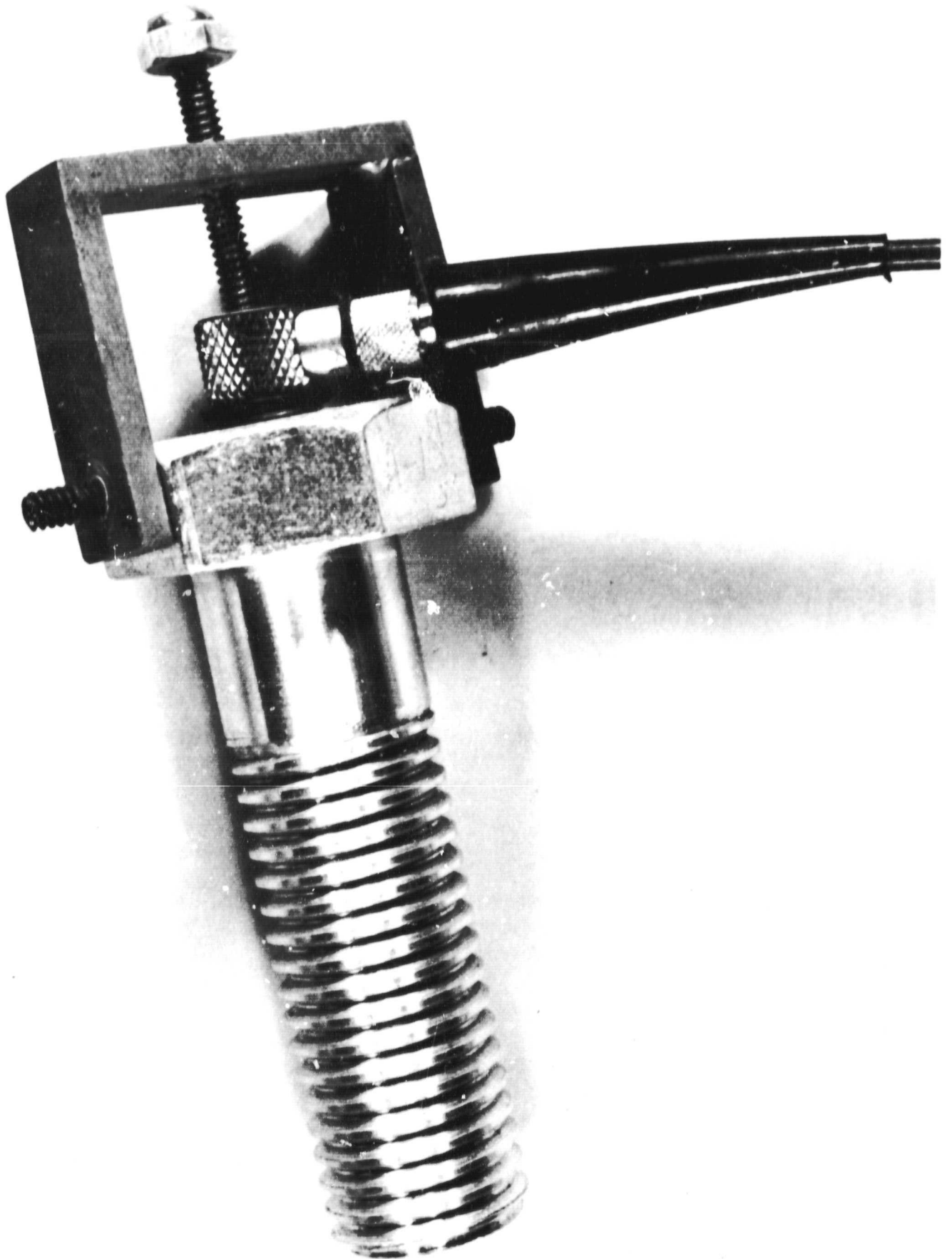


Figure 7 - MRI-1 Aluminum Bolt With Transducer Held
in Place With Yoke Arrangement

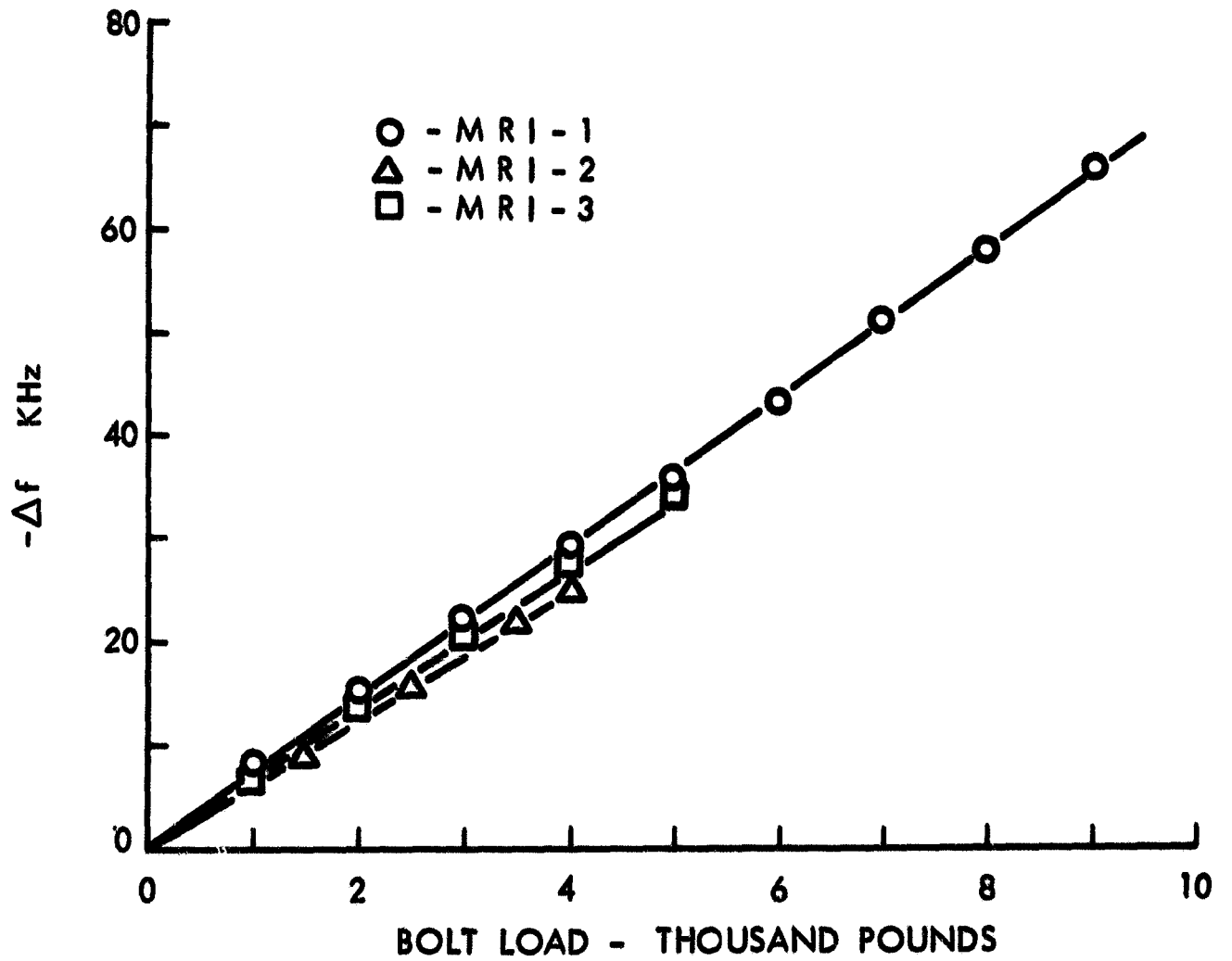


Figure 8 - Frequency Change Vs. Bolt Load for Three MRI Bolts

The sign of Δf as indicated in Figure 8 is negative. Similar results were obtained for all of the bolts examined. Thus, as a bolt is loaded in tension the frequency of a given null decreases. This frequency decrease is in agreement with the increased length but, as mentioned previously, the sign of the velocity change is difficult to predict unless the so-called third-order elastic constants are known. This is not too important since we are not able to separate the effects of ΔL and Δv , but the general observation that f normally decreases with tensile load does indicate that the Δv effect is either additive to the ΔL effect, or at least smaller in magnitude.

It can be noted from Figure 8 that for MRI-1 Δf is almost 70 KHz for a load of 9,000 lb., a reasonably typical load for this bolt. Since the null frequency at zero load and 9,000 lb. can each be reproduced to within 100 Hz, the reproducibility of Δf should be to within approximately 200 Hz, i.e., equivalent to an error of only about 0.3%. There are, of course, other factors which may increase this error but the measurement technique itself has high inherent accuracy. Some of the extraneous sources of error have been investigated and are discussed in the following sections.

A. Transducer Coupling

It is possible to couple ultrasonic waves from a transducer directly to an optically flat surface without any intermediate coupling agent. However, for the application at hand it is essential that some intermediate couplant be used. During the first six months of this program numerous coupling methods were investigated including noncontact techniques with an intermediate water path and contact techniques utilizing a wide variety of greases, oils, and water. The contact technique appears to be the most promising. Greatest reproducibility has been achieved using a silicone vacuum grease.

The grease couplant, of course, contributes to the round trip transit time of the ultrasonic signal. This contribution is small, generally much less than one period of the ultrasonic frequency, but it cannot be ignored in very precise measurements, especially if absolute values are of interest. Fortunately, such absolute measurements are not required in the frequency-null evaluation of load during assembly. As long as the thickness of the couplant doesn't vary during the bolt tightening process the bond contributes very little error to Δf readings. In fact, we have found that for a given bolt the transducer can be removed and replaced many times and the Δf versus load readings are reproducible to approximately $\pm 1\%$.

The effect of the couplant is much more troublesome when the ultrasonic load measurements are made subsequent to assembly. In this application we come closer to a need for absolute rather than relative measurements. Thus, the absolute frequency of a given null must change very little from one bond to another. This variation has been investigated and found to be about $\pm 3\%$ on surfaces that are reasonably smooth and flat (400 grit finish). The reproducibility deteriorates with increasing surface roughness. Other factors, more important to the post-assembly load analysis problem, are discussed elsewhere in this report.

B. Bolt-End Surface and Geometry

Optimum ultrasonic measurements are generally obtained on specimens with opposing surfaces flat and parallel. These ideal conditions cannot be expected in most bolts, so some indication of reproducibility is needed for non-ideal conditions. We have tried to obtain such data in a systematic investigation of both specially prepared and "as received" bolts. The results of this study indicate that non-parallelism of the bolt ends is less troublesome than we expected. Several aluminum bolts of MRI-1 configuration were prepared with the head and end surface out of parallel by various degrees. With non-parallelism ranging from 0 to 20 min., the Δf values for 10,000 lb. loads varied by only $\pm 1\%$. Some of these same bolts were then examined in the "as received" condition (except that the previously mentioned metal bump on the head was removed) and the data scatter was still less than $\pm 2\%$.

Statistical data were also obtained on some of the 3/8 in. mild-steel bolts (MRI-2) in the as received condition. Here the experiments were performed using a transducer-wrench tool in a way that simulated actual assembly procedures (see Section VI) and the scatter was $\pm 5\%$. The experiment was repeated on the same bolts after the ends were ground flat. The load values were then confined to a range of $\pm 2\%$. The grinding operation was performed by a hand-held technique, without any extreme care to insure parallelism.

Both of the bolt configurations mentioned above (MRI-1 and MRI-2) had simple hex heads that were reasonably flat. Many bolts have identification or alloy numbers stamped or embossed on the head. If such figures interfere with an intimate flat contact between the transducer and the bolt head, significant errors can be expected. The interfering characters should be avoided or removed where high precision is desired.

C. Length

Expressions (1)-(3) clearly indicate that the slope of a Δf -versus-stress curve should depend on both the total length and the stressed length of a bolt. Experimental confirmation of this dependence was obtained through a series of experiments where the total length and the stressed length were varied. The results of one such experiment are shown in Figure 9. All of these data are from the same MRI-1 type bolt whose overall length was approximately 3 in. and whose stressed length was varied by changing the nut position along the threads. Between each set of data the stressed length was changed by approximately one revolution of the nut or 0.1 in. The load was applied hydraulically so that for a given nut position thread travel was eliminated during the loading cycle. It is quite clear that the slopes of the Δf -versus-load curves increase significantly as the stressed length is increased. Similarly, Figure 10 shows the effect of changes in total bolt length when the stressed length is held constant.

The above results emphasize that the stressed length and total length must both be known in order to determine the load or stress level represented by a given Δf value. However, the accuracy required in estimating these lengths is not great, so compensation should not be too difficult. It is possible that the readout equipment in a final prototype could automatically correct for bolts of different configuration and application.

It should be recognized that some change in the stressed length occurs during assembly. As the nut on a bolt is tightened by rotation, thread travel results in a reduction of the stressed length. Thus, the estimate of stressed length should be made for the desired state of stress.

D. Temperature

Two different temperature effects were investigated as potential sources of error. The derivations of Appendix A clearly indicate that the frequency of a given null is dependent on any external variable which affects either the length of the bolt or the velocity of ultrasonic propagation. Temperature will affect both of these parameters. Figure 11 shows the effect of temperature on two of the bolts supplied by NASA. The frequency changes shown are due to temperature-induced changes in length and velocity. The slopes of the two curves are quite different, just as the Δf -versus-stress relationships are different for these same bolts. Over the temperature range represented in Figure 11 the change in frequency is by no means small when compared with the stress-induced effects. During the actual tightening of a bolt the expected temperature change will be quite small.

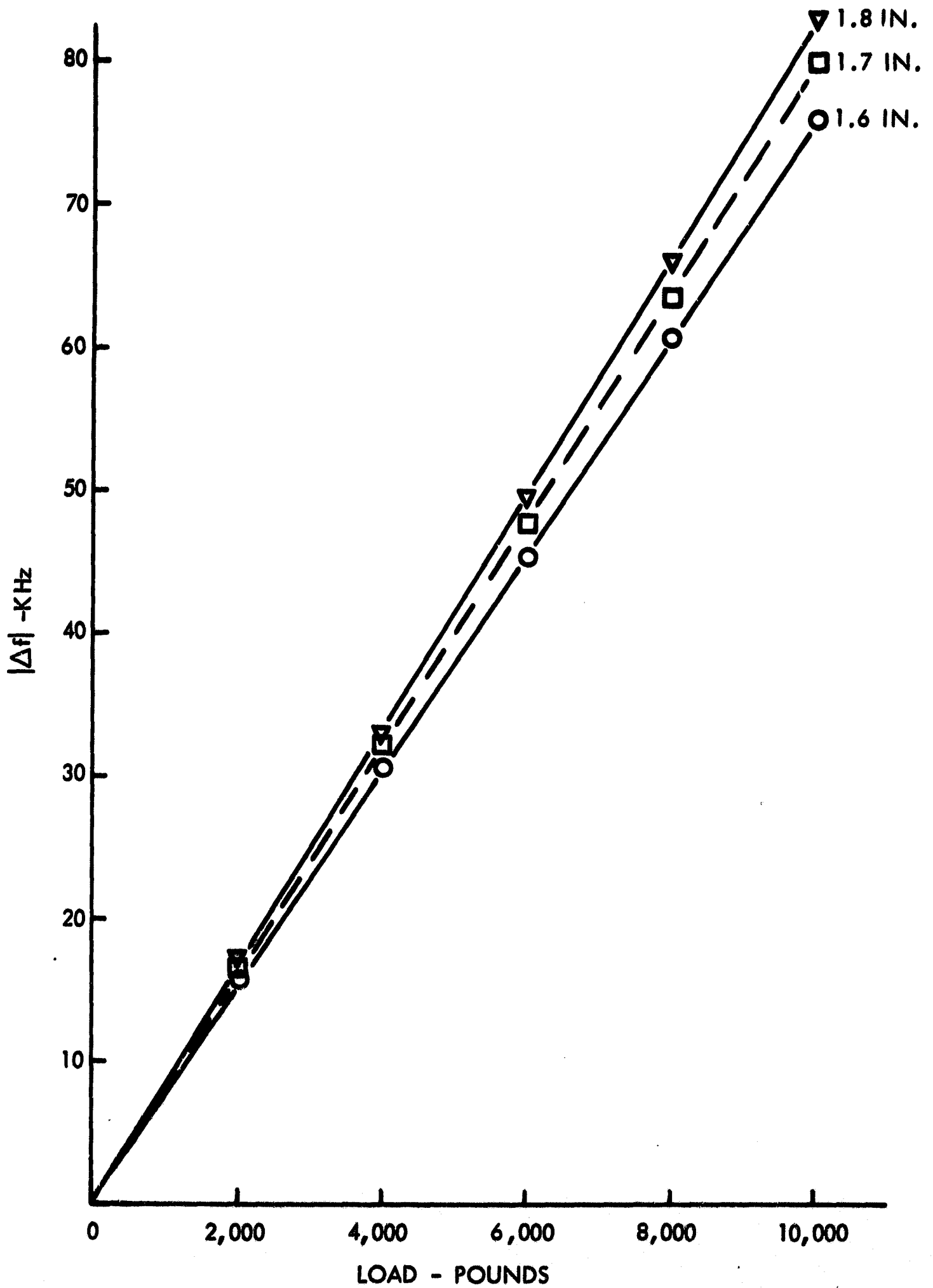


Figure 9 - Response Curves for an Aluminum Bolt With Indicated Stressed Length

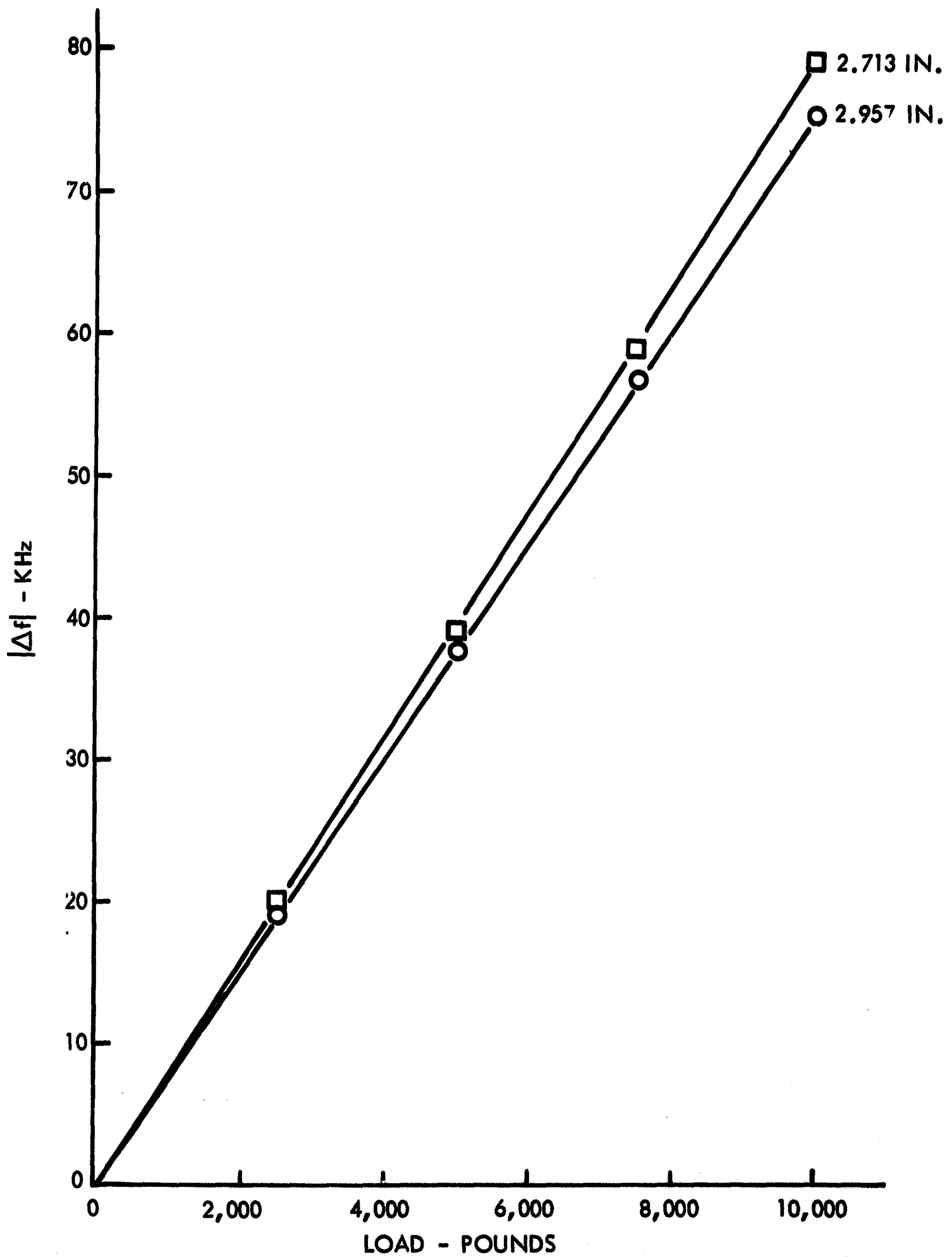


Figure 10 - Response Curves for Two Aluminum Bolts of the Same Stressed Length but With Different Real Length as Indicated

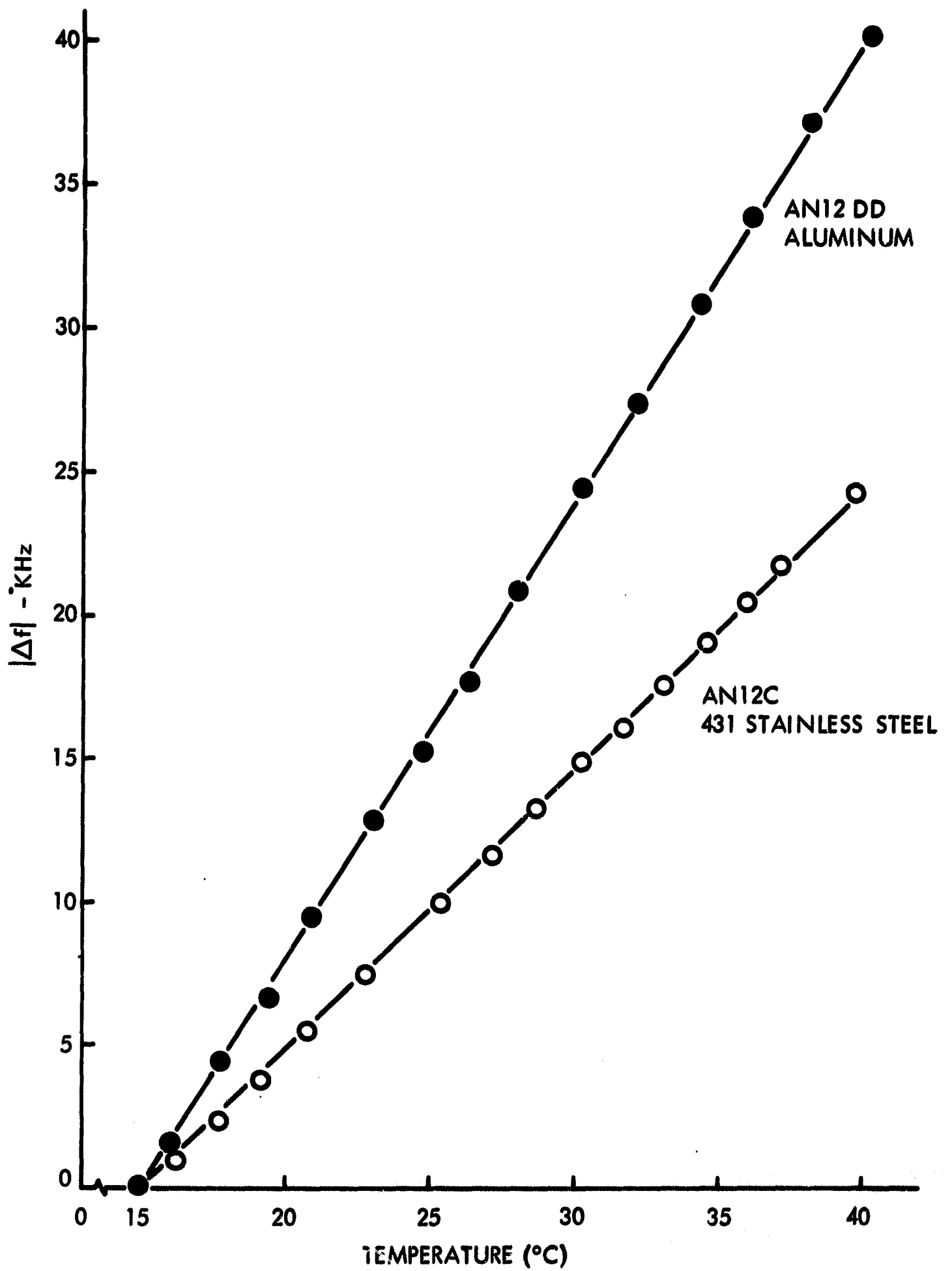


Figure 11 - Changes in Null Frequency Versus Temperature for Two NASA Supplied Bolts

However, significant temperature changes may occur between assembly and post-assembly measurements. Thus, temperature corrections would probably be required for post-assembly load checks.

The second temperature effect investigated was the influence of temperature on the frequency-versus-load response. To examine this effect we studied an MRI-1 aluminum bolt at two temperatures which differed by almost 40°C. The results are shown in Figure 12. It is quite satisfying to see that the change in response over this relatively wide temperature range is quite small. In fact, the minor differences are probably due to a change in temperature that occurred during loading at the lower temperature. Thus, it appears that for assembly type measurements the temperature should present no serious difficulties so long as the temperature remains reasonably constant ($\Delta T \leq 1^\circ\text{C}$) during the short period while the bolt is being tightened and the frequency null measurement is taken.

E. Plastic Yielding

For the data presented thus far, the bolt stresses did not exceed the yield strength. Thus, the unloading portion of a Δf -versus-load plot closely retraces the straight line load curve and returns to the initial condition. However, when the yield point is exceeded, the results are quite different, as illustrated in Figure 13. Plastic deformation causes the slope to increase rapidly (primarily due to the change in length) and prevents the unloading curve from retracing the loading curve. However, the entire unloading curve approximates a straight line with a slope almost equal to that of the elastic portion of the loading curve. The overall response is very similar to that shown in an ordinary stress-strain curve where plastic deformation is present. Under these conditions, the frequency is multivalued in stress and ambiguity in stress analysis is therefore possible. However, it is also clear that the ultrasonic technique might be useful in detecting plastic deformation, a factor that is not easily detected with ordinary torque wrenches.

The effect of yielding was also investigated in an experiment in which three identical MRI-1 bolts were subjected to different loading conditions. The results are shown in Figure 14. All three bolts exhibited similar behavior in the elastic region but the extent of the region and the subsequent Δf response was clearly dependent on the loading condition. The bolts fractured at different tensile loads but they all fractured at approximately the same value of Δf , another feature which may be of value in the routine testing of bolts.

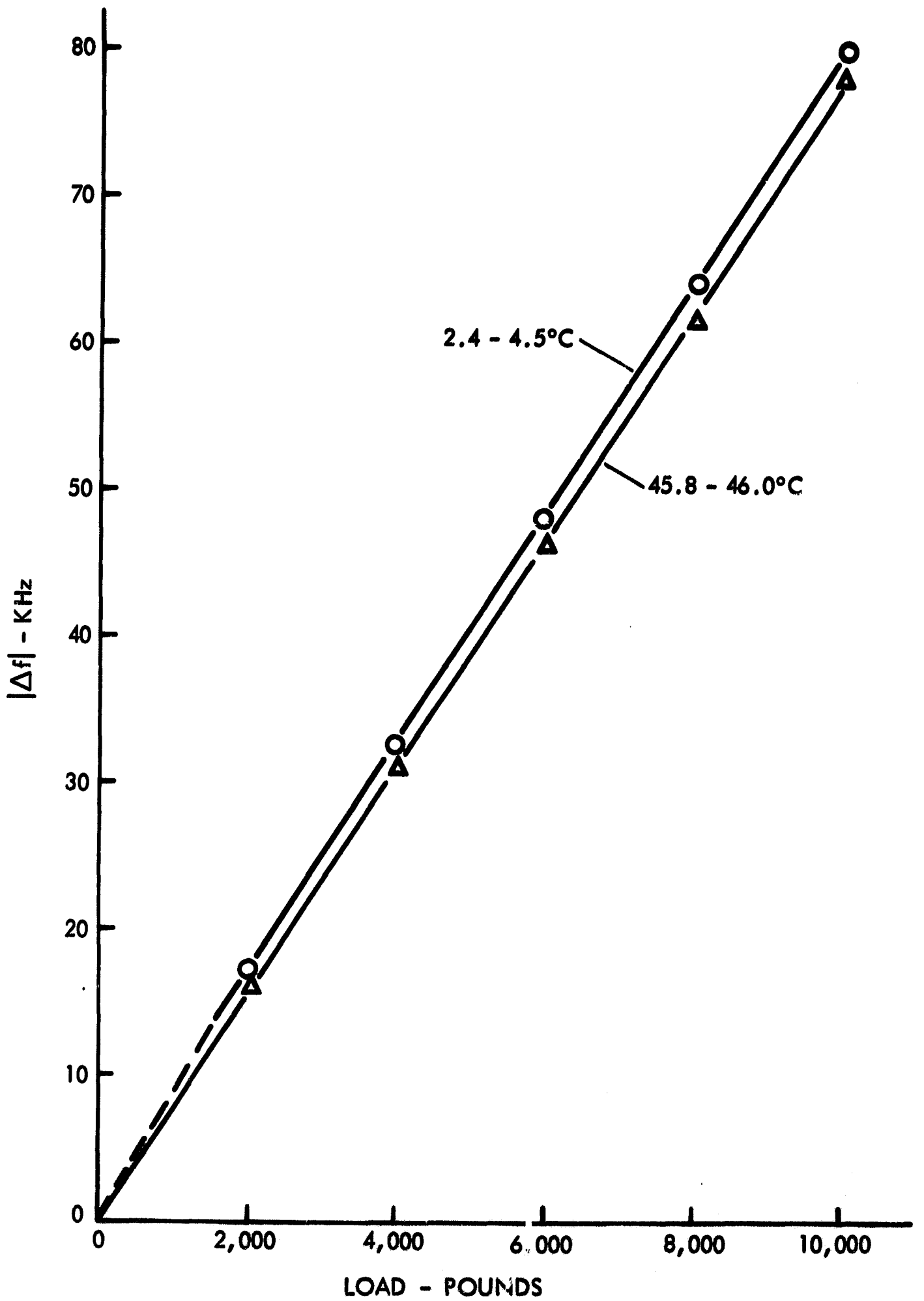


Figure 12 - Frequency Change Versus Load for an (MRI-1) Aluminum Bolt Held at the Indicated Temperatures During the Loading Operation

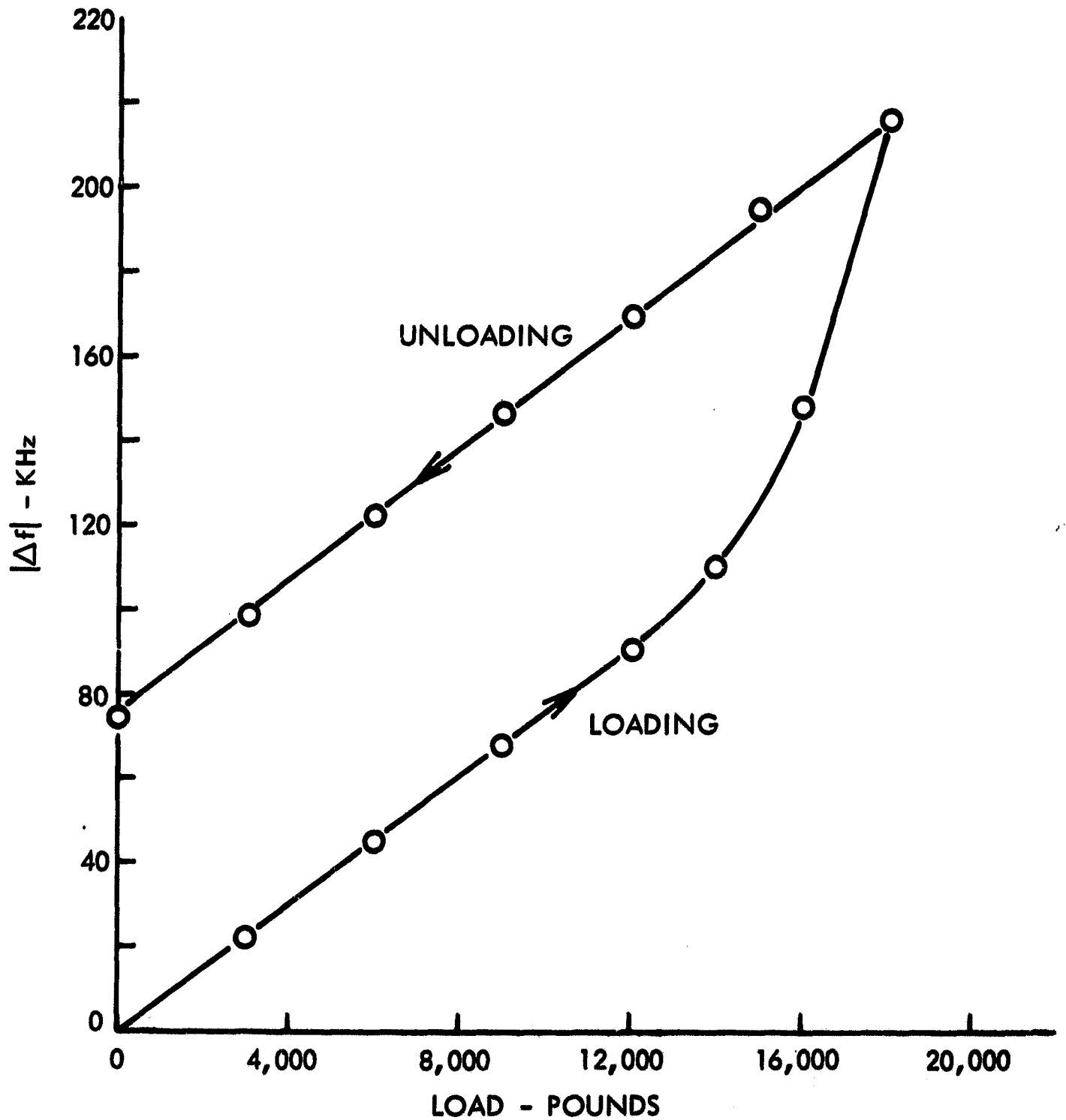


Figure 13 - Loading and Unloading Curves for an Aluminum Bolt Stressed Beyond the Yield Strength

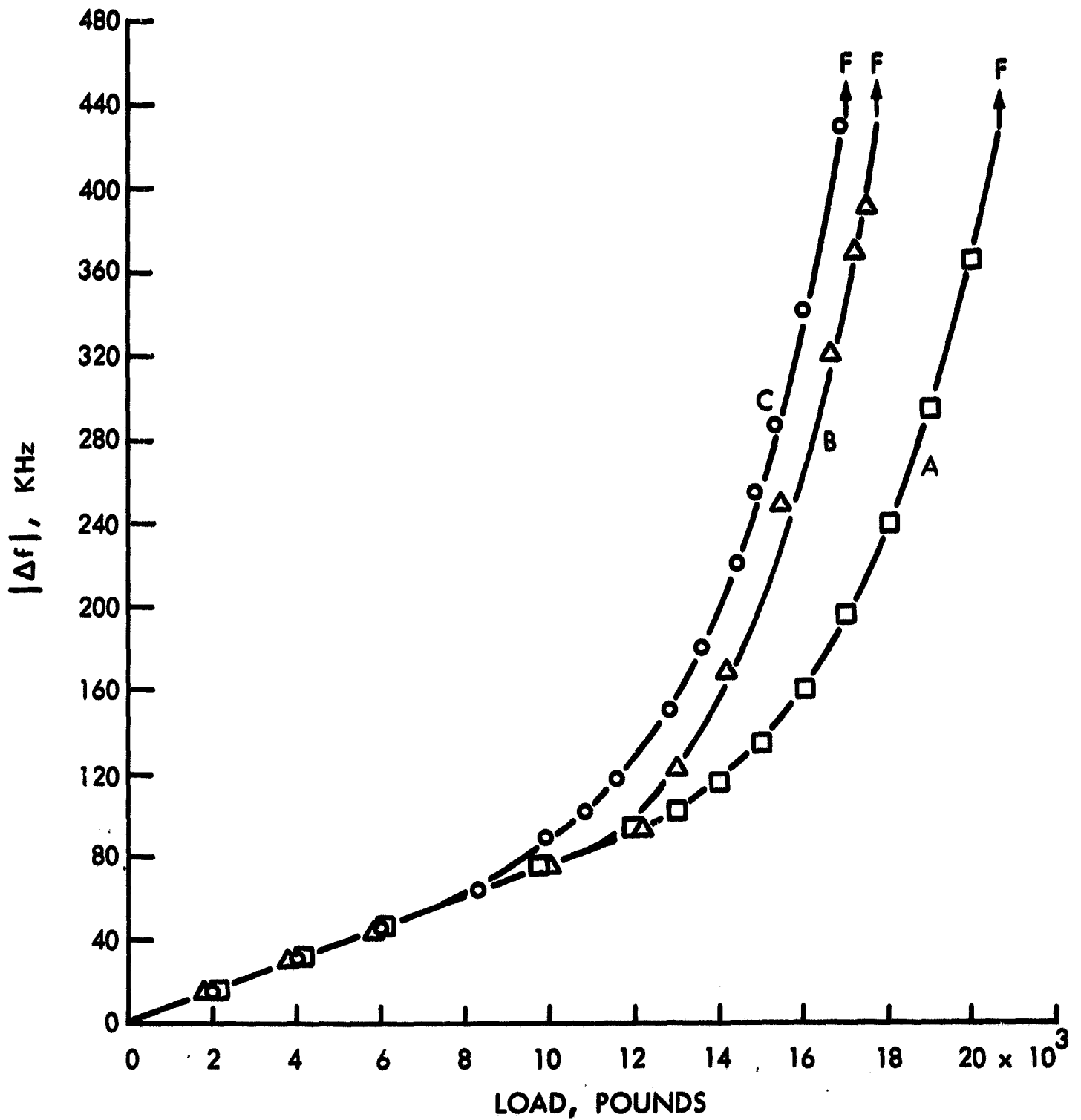


Figure 14 - Frequency Change Versus Load for Three Identical 3/4-In. Aluminum Bolts Loaded in (A) Pure Tension, (B) Torque-Tension with Threads Lubricated and (C) Torque-Tension Without Lubrication. Fracture, Symbol F.

The above results indicate that plastic yielding shouldn't interfere with the anticipated use of the frequency-null technique in load analysis during assembly. In fact the technique could be of considerable value in detecting such yielding, which normally is undesirable. However, like temperature changes, excess stressing after assembly, during static firing for example, would change the pre-assembly reference null and make post-assembly analysis more difficult.

F. Shear Stresses

The effects of shear stresses on null-frequency measurements are also of interest and have received some attention. Some insight into this problem can be gained by re-examining Figure 14. Note that the Δf -versus-tensile-load response in the elastic region is very nearly the same for all three bolts even though two of them were loaded in torque tension. The torqued bolts were theoretically subjected to maximum shear stresses of approximately 18,000 psi at the upper end of the elastic region. The maximum shear stress level at this point is not too much less than the measured tensile stress.

Additional shear measurements were performed on bolts of both the MRI-1 and MRI-2 configuration. Frequency-null observations were made on the bolts while we attempted to apply pure shear stresses without any tensile load superimposed. In reality, some tensile stresses were probably present due to slight bending which was difficult to completely eliminate. The maximum shear stresses were of approximately the same magnitude as the tensile stresses which previously had produced Δf values of 30-70 KHz. Under nearly pure shear loading the observed Δf values were generally less than 0.7 KHz. Even this small effect was probably due to the slight bending mentioned earlier and discussed in more detail in the next section. Thus, it is our conclusion that pure shear produces an insignificantly small effect on the propagation properties of a longitudinal wave as used in our measurements. This conclusion is in agreement with theoretical predictions.

G. Bending

Another source of error which was investigated is that of bolt bending during the tightening process as might occur in a variety of actual fastener applications. The condition was first simulated by placing steel shimstock under one edge of the bolt head during the loading process. The load was then applied hydraulically. The results of this test are shown in Figure 15. The straight-line response representative of nonbending conditions progressively degenerated as 10, 20 and 30 mil shimstock was placed under one edge of the bolt head. The results seemed to vary most widely

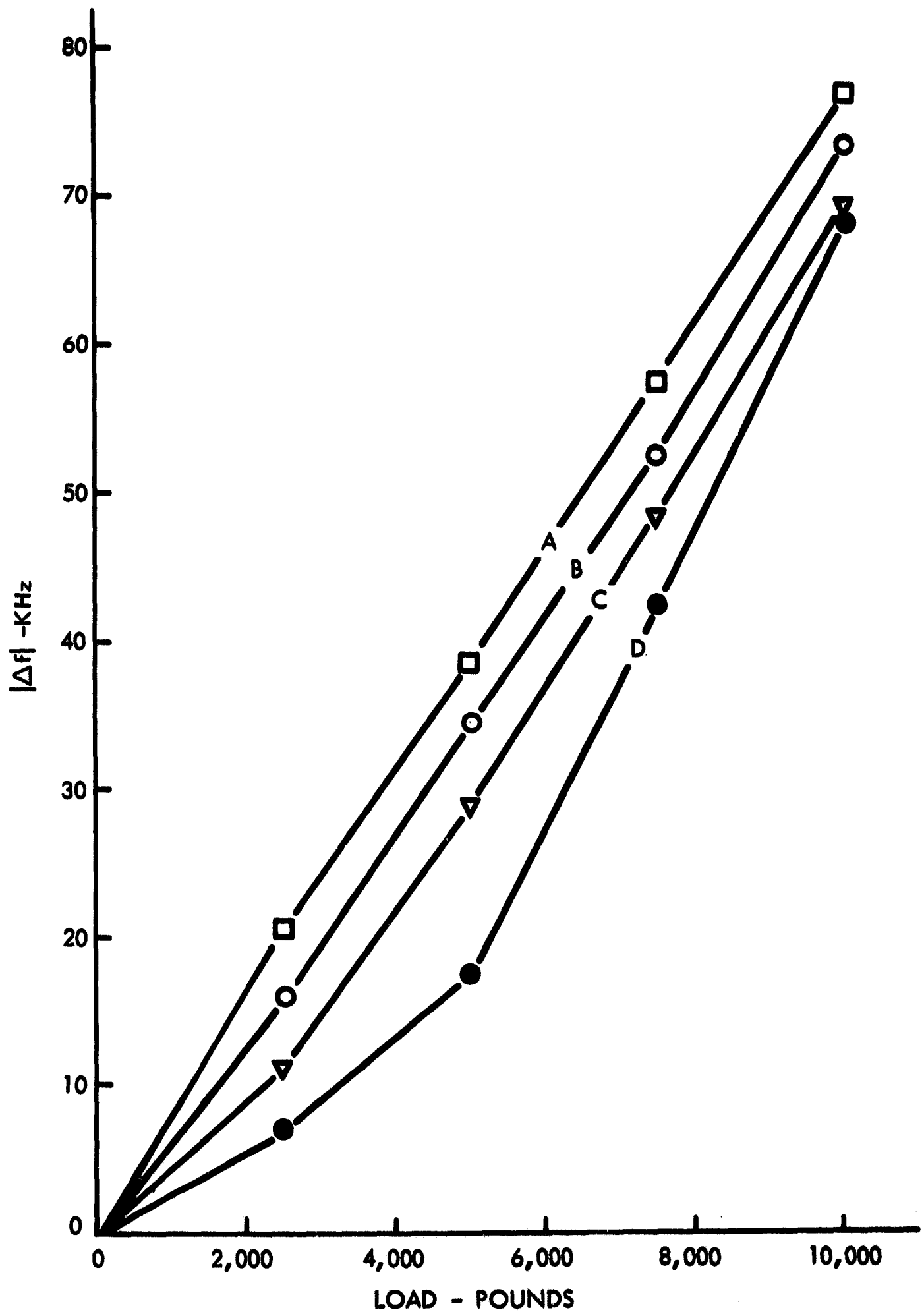


Figure 15 - Frequency-Versus-Load Curves for an Aluminum Bolt With (A) 0 Mils, (B) 10 Mils, (C) 20 Mils, and (D) 30 Mils of Steel Shimstock Under one Side of the Bolt Head to Induce Bending During the Loading Operation

under relatively light load conditions, and then to become somewhat more consistent at the higher loads. The test was not very quantitative but it emphasized the need for further study of the bending effect.

Further testing was accomplished by screwing a short segment of the threaded end of MRI-1 and MRI-2 type bolts into a rigid bar of steel. The bolt head was allowed to protrude from the bar surface by varying amounts. A transverse load was then applied to the head so that the bolt underwent bending in a cantilever mode. A transducer was coupled to the head and frequency-null observations were made during bending. Preliminary results indicated that Δf values of approximately 10 KHz could be created in either MRI-1 or MRI-2 bolts with bending moments of approximately 100 ft-lb. This was initially considered a rather alarming result because 10 KHz represents a very large error compared with the 30 to 70 KHz observed for ordinary tensile loads. Continued investigation revealed that Δf -versus-bending results were quite sensitive to the transducer position on the head of the bolt. We then discovered that the frequency of a given null would increase or decrease during bending depending on whether the transducer was displaced to one side or the other of the neutral fiber of the bending bolt. In addition, the magnitude of the Δf effect was observed to increase as the displacement from the neutral axis increased. With these results we were able to define the primary mechanism by which bending influenced frequency-null measurements. It is simply through the tensile and/or compressive stresses created by the bending. If a transducer is very carefully centered on the head of a bolt with an applied bending force, one-half of the ultrasonic beam travels in material under compression and one-half travels in material under tension. These stresses influence the incremental parts of the beam in exactly the same manner as an applied uniaxial stress. The overall result is that the ultrasonic wave front probably becomes non-planar, or its orientation at least changes with propagation; thus the wave front of a returning echo is not completely parallel to the transducer surface. The electrical signal created by such a wave will be phase shifted from the condition represented by no bending. The magnitude of the phase shift should increase from the no-bend condition as the beam is displaced further from the neutral axis.

With the above mechanism active it is clear that frequency-null measurements should exhibit considerable scatter if bending is present. The errors due to bending can be minimized by centering the transducer on the neutral axis and, with care the total scatter in a series of tests can be held to a few percent. Nevertheless, bending does present one of the largest sources of data scatter. The reason for this becomes quite clear by observing that the maximum fiber stress, in bolts subjected to a bending moment of 125 ft-lb, may exceed the recommended tensile stress. The stresses due to bending are, of course, superimposed upon any tensile stresses due to bolt tightening and the resultant stresses are very inhomogeneous. Although

frequency-null measurements may exhibit data scatter related to the inhomogeneous stresses, it must be recognized that these frequency variations are indicative of true stress variations. It is possible with further development of transducer placement and signal processing that bending effects can be analyzed as well as pure tensile loads.

V. NASA SUPPLIED BOLTS

Of the NASA supplied bolts, shown in Figure 5, the head configurations varied considerably. Because of embossed identification characters and complex heads, one bolt of each type (except those made of 4140 steel) was first prepared by machining the head and threaded ends flat and parallel. For bolts which contained drill holes in either the head or shank, sufficient material was removed to eliminate the hole. The 4140 steel bolts were not prepared in this manner because of the internal wrench head; however, the bottom of the wrench hole was flattened with an end mill. These rather idealized conditions were created in order to evaluate the Δf -versus-load characteristics of each bolt without undue influence from extraneous geometrical factors.

The Δf -load characteristics of the four 3/4 in. bolts are shown in Figure 16. Although the data presented in Figure 16 have not been normalized to a constant value of l_s/l_t , such a correction would not effect a major change in any of the four response curves. Aluminum is obviously the most sensitive material with the three steels all exhibiting significantly smaller slopes.

The response curves for three of the smaller bolts are plotted in Figure 17. Even in these smaller bolts reasonably satisfactory results were obtained by simply using silicone vacuum grease to couple the housed transducer to the bolt head. Using this technique we were able to examine all of the NASA supplied bolts (after end machining) except MS 20004-10, the 1/4 in. bolt with an internal wrenching head. After testing different size bolts of each alloy, the load data were converted to stresses and the curves of Figures 18 and 19 were obtained. For each of five alloys, Δf is plotted against several calculated stress levels to which each bolt was tested. Theoretically, all of the data points should fall on a straight line passing through the origin. However, some deviation from this ideal can be traced to the fact that all stress calculations were based on the diameter of the bolt shank and no consideration was given to the two stress areas discussed earlier in this report. Under these conditions the results are rather impressive. It is desirable to achieve good agreement of Δf -versus-stress for different bolts of a given alloy because this will facilitate the extrapolation of a single calibration test to bolts of widely varying sizes.

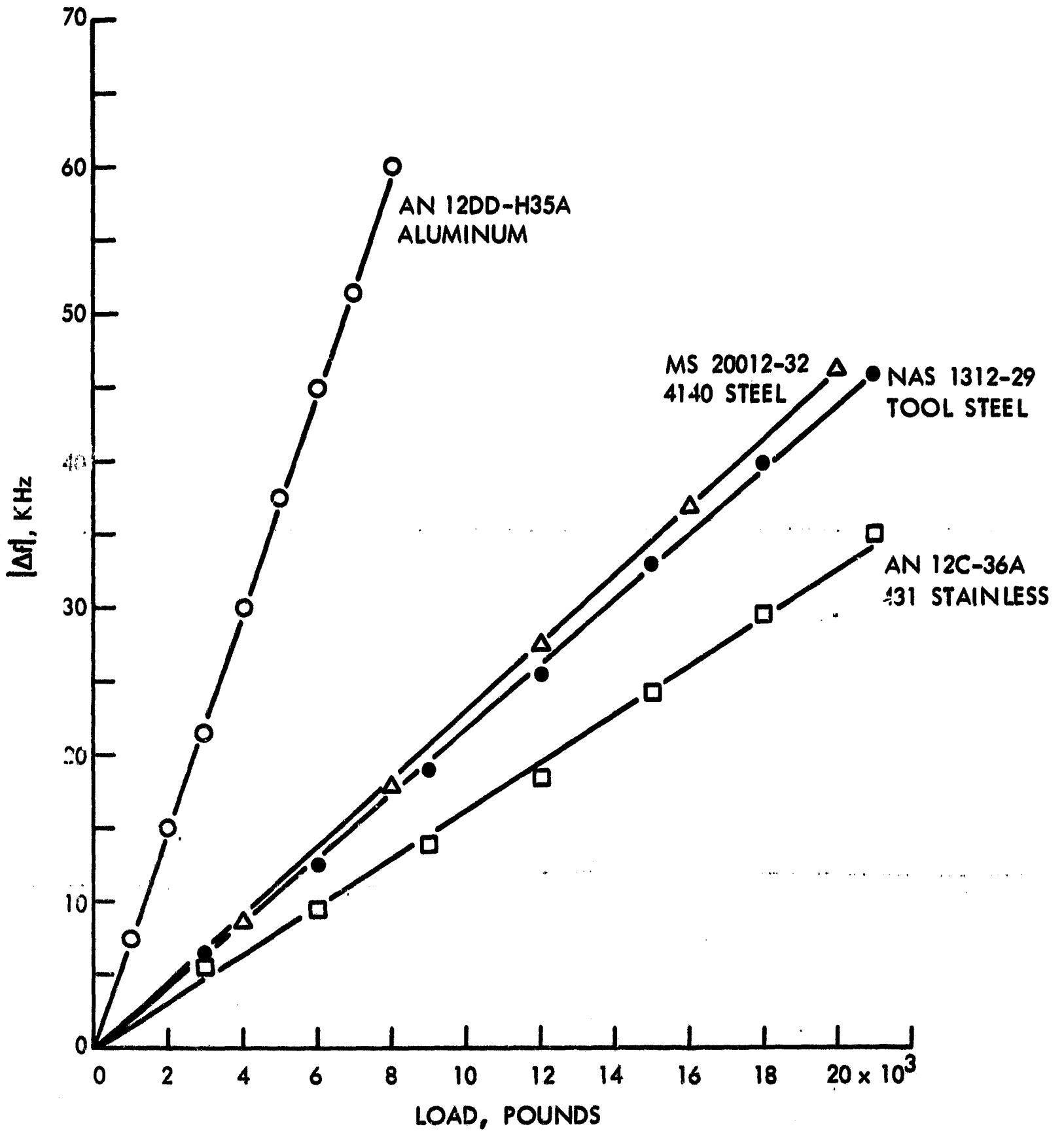


Figure 16 - Frequency Change Versus Load for Four NASA-Supplied Bolts.
 All are 3/4-in. bolts with head and threaded ends machined flat and approximately parallel.

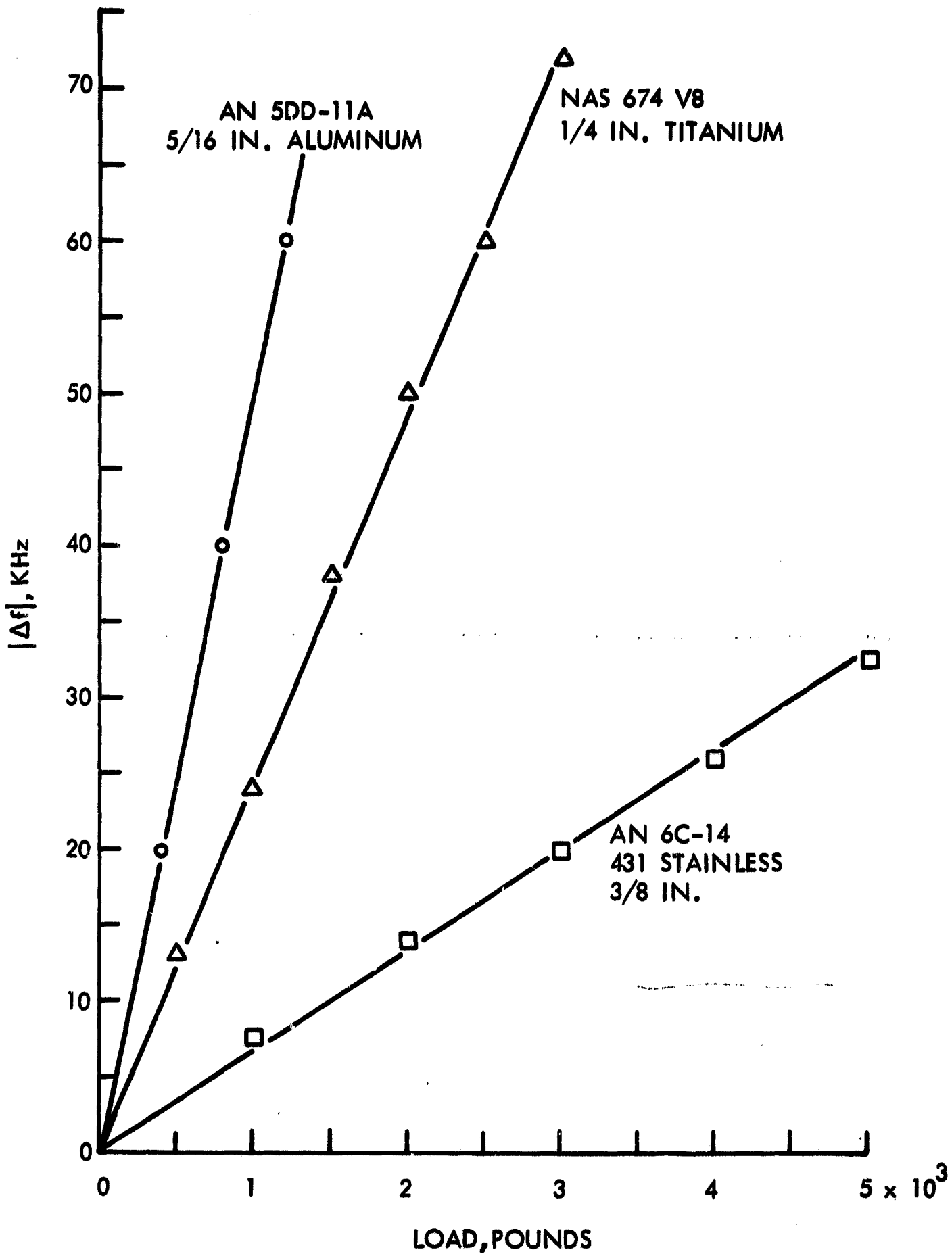


Figure 17 - Frequency Change Versus Load for Several Different Bolt Sizes and Alloys. Head and threaded end were machined flat and parallel on all bolts.

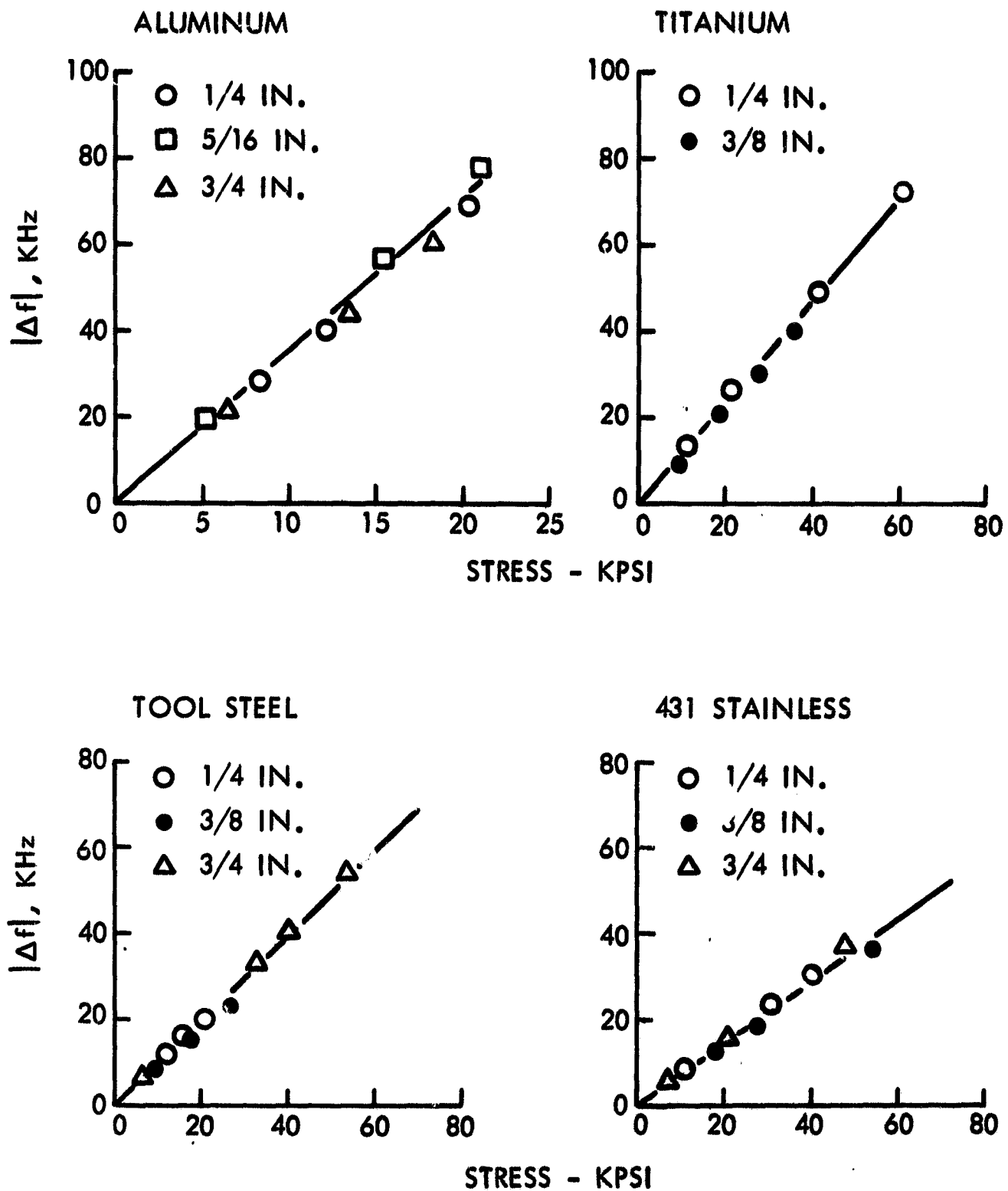


Figure 18 - Normalized Frequency Change Versus Stress for NASA-Supplied Bolts. Head and threaded ends were machined flat and parallel.

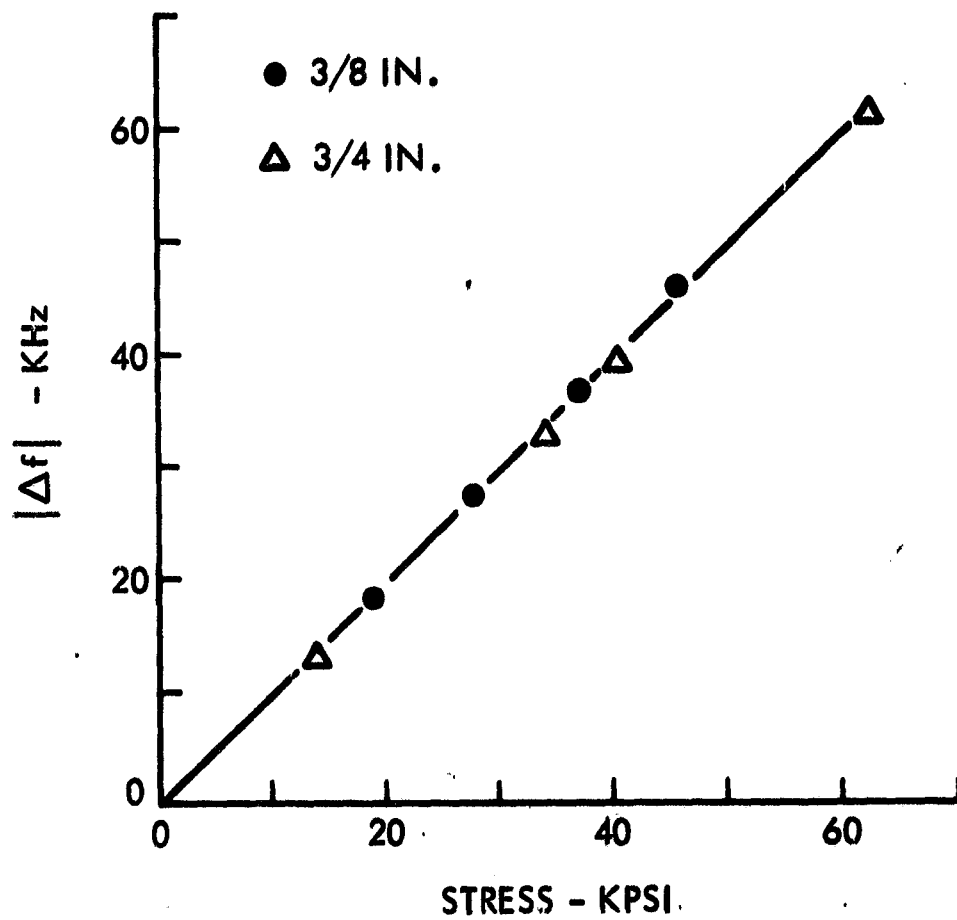


Figure 19 - Frequency Change Versus Stress for 3/8-in. and 3/4-in. Bolts of 4140 Steel.

Examination of Figures 18 and 19 reveals that a given stress produces the largest Δf in aluminum and the smallest in 431 stainless steel. The results for the two other steels and titanium are all very similar.

In addition to the investigation of NASA bolts with machined ends, some preliminary results have been obtained from bolts which were examined in the as-received condition. Figure 20 contains results for two such bolts. The aluminum bolt had a fairly smooth, flat, hex head which facilitated direct coupling. Relatively good ultrasonic echoes and nulls were obtained with this bolt even though a drill hole (~ 0.08 in. dia.) runs completely through the hex head. The hex head on the tool steel bolt is recessed with a segment of a spherical surface. As yet we have not been able to couple the ultrasonic beam into this complex head shape so the tool steel bolt was examined by coupling directly to the flat threaded end. The echoes obtained in this case were not ideal but the results are encouraging nevertheless.

We were also able to examine both of the titanium bolts and the $3/4$ in. stainless bolt in the "as-received" conditions. All of the remaining NASA bolts defied examination in the as-received condition. However, most of those with otherwise flat hex heads could be examined if the embossed identification numbers could be removed. The primary requirements are a small flat area on the head (approximately $5/16$ in. dia.) with the threaded end also reasonably flat, i.e., somewhat similar to the surface finishes on AN 12DD-H35A bolts.

VI. POTENTIAL FIELD TECHNIQUES

Some project activity has been directed toward transducer application techniques that are compatible with mechanical tools and procedures that simulate normal assembly operations.

We attempted to incorporate the ultrasonic transducer into a socket wrench so that the ultrasonic Δf data could be taken without special jigs, etc. Our first model involved a spring loaded arrangement with the active transducer installed as a part of the socket wrench, as shown in Figure 21. When the socket wrench is placed over the bolt head, the transducer is automatically positioned and pressed against the hex head surface. Coupling of ultrasonic energy into the bolt, of course, requires the use of grease or some other suitable material which can be applied to either the bolt or the transducer prior to placement of the wrench-probe assembly. This technique provided reasonably good echo patterns so long as the socket wrench was not moved. However, when the wrench was actually used to tighten the bolt, we found that the normal wrench wobble, which occurs during this

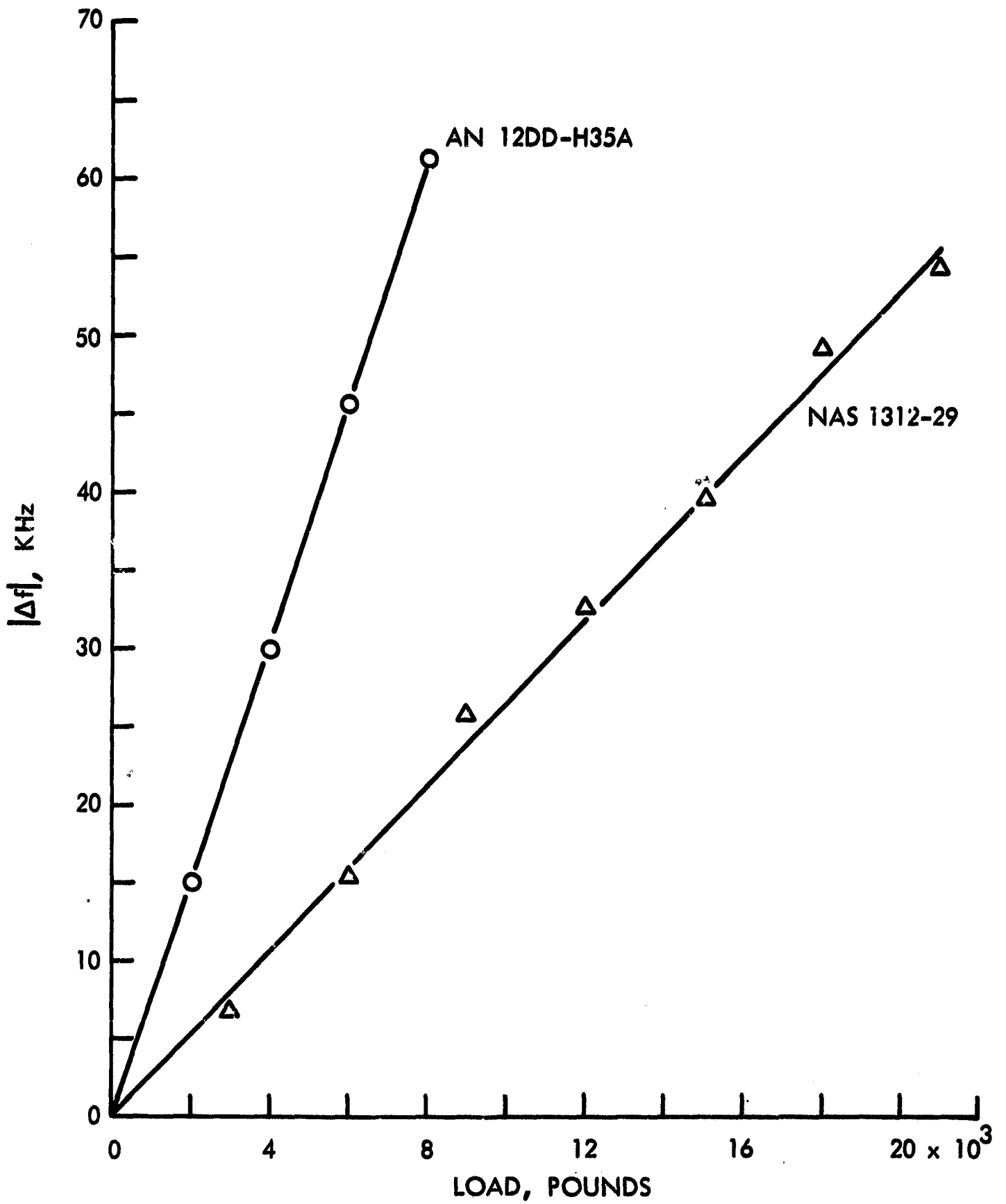


Figure 20 - Frequency Change Versus Load for 3/4-In. Aluminum Bolt, AN 12DD-H35A, and 3/4-In. Tool Steel Bolt, NAS 1312-29. Both bolts were examined in the "as received" condition.

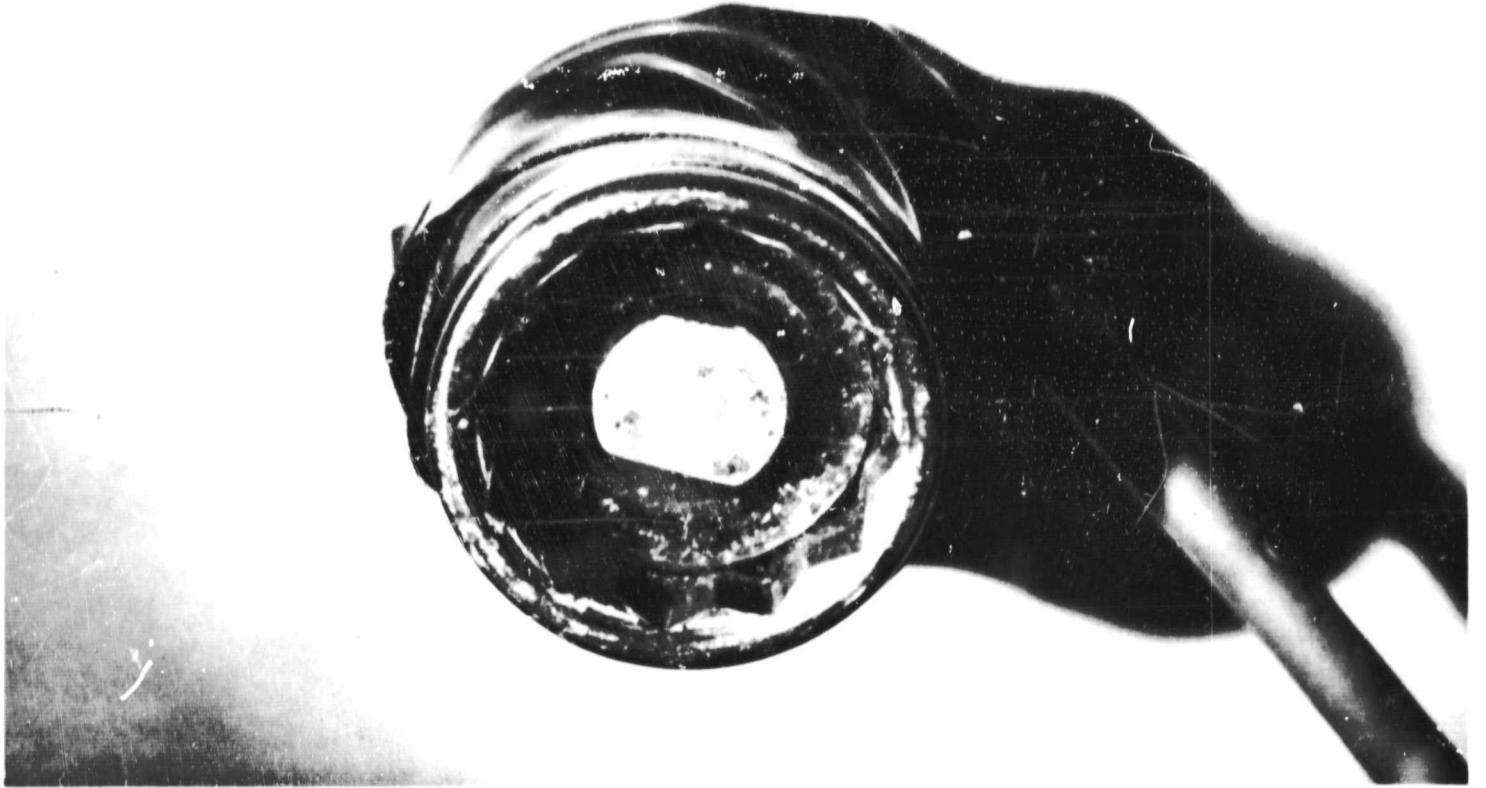


Figure 21 - Prototype Socket Wrench With Spring Loaded Transducer (top) and Modified Socket Wrench With Electrical Contact for Separate Transducer (bottom)

operation, also affects the ultrasonic echoes. The observed changes were due to small, but undesirable, movement of the transducer. Some success in reducing this problem was achieved by decreasing the mechanical coupling between the transducer and the wrench head, but further improvement will be necessary (and can probably be achieved) if the transducer is to be satisfactorily incorporated into the wrench body.

A second approach to the transducer-wrench assembly produced much better results. For this technique a small uncased transducer is first greased onto the bolt head then electrical connections are automatically made when a modified wrench head (as shown in Figure 21) is applied. Using such arrangements the bolt can be completely tightened with practically no adverse effects on the ultrasonic measurements. It is perhaps a slight disadvantage to have to handle the transducer independently; however, some compensating advantages which occur are: (1) the uncased transducers are much less expensive than cased units, and (2) they facilitate selection of several different ultrasonic frequencies without having a special wrench head for each.

Several experiments were performed using the separate transducer and wrench assembly to simulate actual bolt tightening operations and at the same time to analyze load conditions. Figure 22 shows the frequency-null equipment in use for such tests. In order to perform the experiment on several bolts of a given alloy and configuration, we selected a standard 3/8 in. mild-steel, hex head bolt, which was available in quantity (MRI-2). After a suitable calibration we selected a Δf value of 30 KHz, corresponding to a load level of approximately 4,900 lb. Five different bolts, all in the as-received condition, were then tightened to a level determined by ultrasonic readings as follows. The frequency-null condition was first established while the bolt was in the zero stress condition; then the frequency was decreased by 30 KHz. The bolt was then tightened until the null condition was reestablished at the lower frequency. After the load level was artificially determined by ultrasound, the real load level was noted by reading the torque-tension gages. When the bolts were used in the as-received condition, the actual load levels varied over a range equal to approximately $\pm 5\%$ from the average. The experiment was repeated on the same bolts after the ends were ground flat and the load values were then confined to a total range of about $\pm 2\%$. The grinding operation was performed by a simple hand-held technique, without any extreme care to insure parallelism. The results indicate that accuracy can be increased with only modest improvement over the as-received condition.

In performing the above experiment, we recognized a very desirable modification which should be included in the final prototype, e.g., an automatic gain-control circuit which would maintain a constant amplitude relationship between the first ultrasonic echo and the CW reference signal.

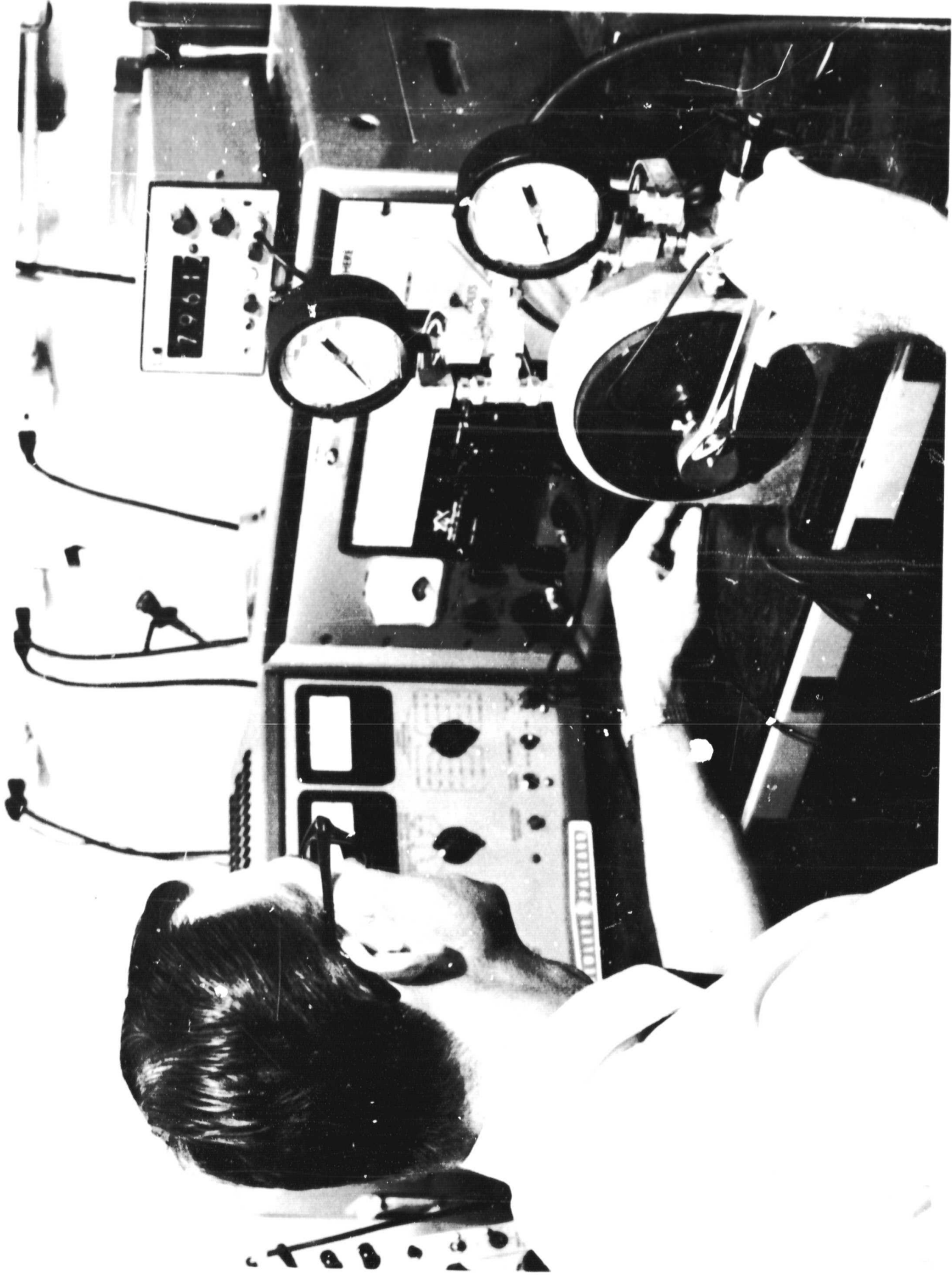


Figure 22 - Photograph of Bolt Being Tightened in Torque Tension Tester and the Load Being Analyzed With the Frequency Null Equipment

VII. CONCLUSIONS AND RECOMMENDATIONS

The results obtained during Phase I of this program indicate that the ultrasonic analysis of bolt loads during assembly (tightening) is definitely feasible. Accuracies well in excess of those obtained with torque wrenches are achievable. In addition, ultrasonic techniques might provide useful information on plastic yielding and bending. Satisfactory results can be obtained on some simple bolts in the as-received condition. However, bolts often have identification numbers or non-flat head configurations which make ultrasonic analysis difficult, if not impossible. Only slight modification of most of these bolts would facilitate ultrasonic examination. For example, the only modification required for many hex head bolts would be removal of embossed identification numbers on the head. In general it is desirable to have a small flat area ($\sim 5/16$ in. dia.) on the bolt head. Accuracy will also improve with the flatness and parallelism of the opposing threaded end but close tolerances are not necessary as illustrated by the results obtained with some of the as-received bolts. With only slightly modified bolts ultrasonic analysis of loads should be possible with errors of only a few percent.

The analysis of loads subsequent to assembly is a much more difficult task. An ultrasonic solution to this problem would require extremely tight tolerances on bolt dimensions and/or record keeping of results before and after assembly. Correction for temperature changes would also be necessary. These requirements will be defined in the final report.

One area of investigation originally planned for Phase I was the effect of material variations between bolts of different lots. This study was not carried out because the lot origin of the NASA supplied bolts could not be definitely established. However, we currently believe that as long as the alloy designation and heat treat condition are specified the ultrasonic variations between lots will be small compared to other sources of error. This fact can be confirmed in Phase II if bolts can be supplied from lots that are known to be different.

It is difficult to extrapolate limited laboratory results into estimations of system accuracy under conditions similar to those encountered in space vehicle assembly. In Phase II we hope to use known dimensional tolerances on bolts and anticipated variations in stressed length, bending conditions, etc., to obtain a better estimate of the accuracy levels possible under field conditions. However, based on results obtained in Phase I we believe that the probable errors of ultrasonically determined assembly loads can be held to less than 3%. To accomplish this the stressed lengths must

be held constant or be determined to within about $\pm 1\%$. For a stressed length of 1 in. the permissible variation would be 10 mils. Evaluation of the actual stressed length may not be necessary if a calibration test can be run for each bolt application where high precision is required. The load length for the calibration test would duplicate the load length for the application of interest.

Temperature variations produce no problems in assembly load measurements if the bolts are in thermal equilibrium with their surroundings. The influence of bending can be minimized by centering the transducer on the bolt axis. Methods of improving the centering accuracy will be investigated in Phase II and details presented in the technical manual.

In laboratory tests where ultrasonic measurements can be made concurrent with load measurements the deviation of Δf -versus-load plots from linearity gives a very accurate indication of the onset of plastic yielding. In actual assembly operations the detection of yielding can only be accomplished indirectly from Δf -versus-load calibration charts obtained under similar loading conditions. These requirements will be discussed in the final report.

Considering the promising results obtained during Phase I of this contract we recommend continuation into Phase II. We believe that further testing of NASA supplied bolts should be done after slight bolt modifications which would facilitate inspection, improve accuracy, and provide quantitative data which has been statistically verified. These modifications can be performed at MRI and would involve the following:

Titanium bolts
NAS 676 V8
NAS 674 V8

Remove identification numbers
and improve flatness of threaded end
(RIN - IFOTE)

Aluminum bolts
AN 12DD-H35A
AN 5DD-11A
AN 4DD-10A

No modification necessary
RIN - IFOTE
RIN - IFOTE

431 Stainless bolts
AN 12C-36A
AN 6C-14
AN 4C-10

RIN-- IFOTE
RIN - Shorten threaded end to eliminate
wire hole
RIN - Shorten threaded end to eliminate
wire hole

4140 Steel bolts

MS-20012-32

Machine flat bottom in wrenching hole

MS-20006-14

Machine flat bottom in wrenching hole

Tool steel bolts

NAS 1312-29

Machine small flat area in center of

NAS 1306-8

head and improve flatness of threaded

NAS 1304-8

end

The only NASA supplied bolt not included in the above list is the 1/4 in. 4140 steel bolt. The wrenching hole in the head of this bolt is so small that it is highly doubtful if a transducer could be introduced for satisfactory ultrasonic measurements. The Phase II report will include the final bolt designs necessary for application of the ultrasonic load analyzer.

The prototype instrumentation to be delivered to NASA at the conclusion of Phase II will be very similar to the equipment described in this report. It will of course be packaged as a single console and some automatic features will be added to facilitate measurements.

APPENDIX A

FREQUENCY-NULI RESPONSE FOR STRESSED BOLTS

Consider the bolt sketch previously shown in Figure 4a where the overall bolt length is l_t . Prior to stress application, the ultrasonic path length would be $2l_t$. Assume that the ultrasonic frequency is adjusted for a null condition which should occur approximately when an integral number, N , wavelengths fit into the total path length. Thus,

$$N = 2l_t f_0 / v_0 \quad . \quad (A-1)$$

There are other factors such as phase changes at the transducer and bolt end which will alter Expression (A-1) but as long as these factors remain constant, the end results of the following derivation will not be affected.

Now assume that the same null is maintained by changing the frequency to f' as a tensile load is applied to the bolt. The tensile load is, of course, only applied over the length l_s , but it produces a change, Δl , in the overall length and a new velocity v' in the stressed region. We can now write

$$N = 2 \left[\frac{l_t - l_s}{v_0} + \frac{l_s + \Delta l}{v'} \right] f' \quad . \quad (A-2)$$

But since the same null condition is maintained, the integer N is the same in (A-1) and (A-2). These expressions can then be equated and we obtain

$$l_t f_0 / v_0 = \left(\frac{l_t - l_s}{v_0} + \frac{l_s + \Delta l}{v'} \right) f' \quad (A-3)$$

which can be simplified to

$$\frac{\Delta f}{f'} = \frac{l_s}{l_0} \left[1 - \frac{v_0}{v'} \left(1 + \frac{\Delta l}{l_s} \right) \right], \quad (A-4)$$

where $\Delta f = f' - f_0$. However, the term $\Delta l / l_s$ is equal to the elastic strain, $\epsilon = S/E$, where S is the stress and E is Young's modulus. We can also write $v' = v_0(1 + \beta S)^{1/2}$ where $\beta = \gamma / \rho v_0^2$ and γ is a constant

for a given material and ρ is the density. For a better understanding of the significance of γ , the reader is referred to the following reference (R. T. Smith, Ultrasonics, 1, 135, 1963). Expression (A-4) can then be written as

$$\frac{\Delta f}{f'} = \frac{l_s}{l_t} \left[1 - \frac{v_0(1+\alpha S)}{v_0(1+\beta S)^{1/2}} \right] \quad (A-5)$$

where $\alpha = 1/E$. Since $\alpha S \ll 1$ and $\beta S \ll 1$, we can approximate expression (A-5) as follows:

$$\frac{\Delta f}{f'} \cong \frac{l_s}{l_t} (\beta/2 - \alpha) S \quad (A-6)$$

Thus, we see that $\Delta f/f'$ is linear with stress, S , and depends on the dimensions l_s and l_t , as well as the material constants, β and α .

For bolts having two different cross-sectional areas within the length l_s (see Figure 4b), it is necessary to write

$$\frac{\Delta f}{f'} \cong \frac{(\beta/2 - \alpha)}{l_t} (S l_s + S' l_{s'}) \quad (A-7)$$

where S is the stress in length l_s and S' is the stress in length $l_{s'}$. Since the stress in each sublength is related to the overall load, L , and the effective cross-sectional area, A , we can alternatively write (A-7) as follows:

$$\frac{\Delta f}{f'} \cong \frac{(\beta/2 - \alpha)}{l_t} \left(\frac{l_s}{A_s} + \frac{l_{s'}}{A_{s'}} \right) L \quad (A-8)$$

In expressions (A-6) through (A-8) the original frequency f_0 could be substituted for f' with little loss in accuracy since they differ by less than one part in 100.

REFERENCES

1. Hughes, D.S., and J. L. Kelly, Phys. Rev., 92, 1145 (1953).
2. Bergman, R., and R. Shahbender, Jour. App. Phys., 29, 1736 (1958).
3. Benson, R.W., and V. J. Raelson, Product Engineering, 30, 56 (1959).
4. Waterman, P.C., and L. J. Teutonico, Jour. Appl. Phys., 28, 266 (1957).
5. McSkimin, H.J., Jour. Acoust. Soc. Amer., 37, 864 (1965).
6. Papadakis, E.P., Jour. Appl. Phys., 35, 1474 (1964).
7. Pervushin, I.I., and L. P. Filippov, Soviet Phys.-Acoustics, 7, 307 (1962).
8. Benson, R.W., and Associates, Inc., NASA Report No. N68-21875 (1968).